Maturation signatures of conventional dendritic cells in COVID-19 reflect direct viral sensing

Laura Marongiu[1,2], Giulia Protti[1,2], Fabio A. Facchini[1], Mihai Valache[1], Francesca Mingozzi[1], Valeria Ranzani[2], Anna Rita Putignano[2], Lorenzo Salviati[1,2], Valeria Bevilacqua[2], Serena Curti[2], Mariacristina Crosti[2], Mariella D'Angiò[3], Laura Rachele Bettini[3], Andrea Biondi[3], Luca Nespoli[4], Nicolò Tamini[4], Nicasio Mancini[5,6], Nicola Clementi[5,6], Sergio Abrignani[2,7], Roberto Spreafico[8], Francesca Granucci[1,2,*]

[1]Department of Biotechnology and Biosciences, University of Milano-Bicocca, Milan, Italy
[2]National Institute of Molecular Genetics "Romeo ed Enrica Invernizzi", Milan, Italy
[3]Pediatric Department and Centro Tettamanti-European Reference Network PaedCan, EuroBloodNet, MetabERN-University of Milano-Bicocca-Fondazione MBBM-Ospedale, San Gerardo, Monza, Italy.
[4]ASST san Gerardo Hospital, Monza, Italy, School of Medicine and Surgery, University of Milano-Bicocca
[5]Laboratory of Medical Microbiology and Virology, Vita-Salute San Raffaele University, Milan, Italy.
[6]IRCCS San Raffaele Hospital, Milan, Italy.
[7]Department of Clinical Sciences and Community Health, University of Milano, Milan, Italy
[8]Institute for Quantitative and Computational Biosciences, University of California, Los Angeles

*Corresponding author. Email: francesca.granucci@unimib.it; granucci@ingm.org

Abstract: Growing evidence suggests that conventional dendritic cells (cDCs) undergo aberrant maturation in COVID-19, and this adversely affects T cell activation. Here, we find that cDC2 subtypes show similar infection-induced gene signatures with an increasing gradient of expression of interferon-stimulated genes from mild to severe patients and a down-regulation of major histocompatibility complex class II (MHC class II) molecules and some inflammatory cytokines compared to the baseline level of healthy donors. In vitro, the direct exposure of cDC2s to the virus recapitulates the type of activation observed in vivo. Our findings provide evidence that SARS-CoV-2 can directly interact with cDC2s and, by down-regulating crucial molecules required for T cell activation, implements an efficient immune escape mechanism.

One-Sentence Summary: Type 2 conventional dendritic cell functions are altered by direct interaction with SARS-CoV-2

Main Text: Clinical outcomes of COVID-19 are highly variable. Patients may show either no/mild symptoms (such as mild fever and cough) or severe respiratory involvement requiring hospitalization. In the most severe cases, Acute Respiratory Distress Syndrome (ARDS) can develop, with high levels of inflammatory hallmarks in the blood *(1)(2)* and diffuse intravascular coagulation (DIC) *(3)(4)*. In a non-negligible number of cases, COVID-19 is lethal *(5)*. Patients presenting severe symptoms show immune dysregulation characterized by excessive release of type 1 and type 2 cytokines *(2)*, and alterations of lymphoid and myeloid populations in the peripheral blood *(6)*.

Cells of myeloid origin play a pivotal role during infections by sensing pathogens, producing inflammatory mediators and by contributing to the activation of adaptive immunity. In this context, dendritic cells (DCs) are particularly relevant since they are specialized in antigen presentation and T cell priming *(7)*.

Conventional DCs (cDCs) have been divided in two subtypes, cDC1 and cDC2, originating from a common precursor (pre-DCs) *(8)(9)(10)(11)*.

cDC1s have a high intrinsic capacity to cross-present antigens, due to the expression of the CLEC9A c-type lectin *(12)*, and activate $CD8^+$, Th1 and NK cells *(13)*. Myeloid cDC2s express different Pattern Recognition Receptors (PRRs) and can promote a wide range of immune responses and especially $CD4^+$ T cell responses *(14)*. Recently cDC2s have been divided in two subsets, DC2 and DC3 *(15)(16)(17)*. DC3s share some characteristics with monocytes, such as the expression of CD14 *(16)*.

Alterations of cDCs have been described in COVID-19 patients, with decreased numbers in the blood *(18)(19)* and reduced functionality, in terms of cytokines production and T cell priming capacity when restimulated in vitro *(20)*. Nevertheless, no specific information is available concerning the impact of SARS-CoV-2 infection on the maturation of DC subtypes. Therefore, a better understanding is mandatory given the specific role of cDCs in the activation and skewing of adaptive immune responses that ultimately may contribute to COVID-19 pathogenesis *(21)*.

In seeking for the impact of SARS-CoV-2 infection on blood DC subtypes, we analyzed peripheral blood DCs from severe and mild COVID-19 patients, according to World Health Organization (WHO) classification. Patients were enrolled from the STORM cohort (see Supplementary Table 1 for the clinical data of the patients) of San Gerardo Hospital in Monza, Italy.

cDC1s were identified as CLEC9A$^+$ and cDC2s as CD1c$^+$FcεRIα$^+$ over the CD11c$^+$MHCII$^+$ PBMCs excluding cells expressing markers for T and B lymphocytes (CD3 and CD19, respectively) and monocytes (CD88 and CD89) *(15)*. CD14 was included in the analysis to identify DC3s *(16)* (**Supplementary Fig. S1 for gating strategies**). Consistent with some studies *(19)* but not others *(6)*, we found a decreasing trend in the frequency of cDC1s, DC2s and DC3s in COVID-19 patients compared to healthy donors (HDs) (**Fig. 1A**). Interestingly, the inflammatory DC3s expressing both CD14 and CD163 showed an increasing trend, differently from the total DC3 population (**Fig. 1A**). This was consistent with the observation that the frequency of inflammatory DC3s increases in the circulation of patients with inflammatory diseases *(15)*.

To perform a systematic characterization of the transcriptional response of DCs to SARS-CoV-2 infection, we analyzed three different single-cell transcriptomic datasets, two publicly available and a newly generated one. The first dataset *(22)* (dataset 1) contains cellular indexing of transcriptomes and epitopes by sequencing (CITE-seq) data of PBMCs and enriched DCs obtained from 12 subjects (7 COVID-19 patients and 5 HDs), while the second dataset *(23)* (dataset 2) contains scRNA-seq data of PBMCs obtained from 18 COVID-19 patients and 21 HDs. The new dataset (dataset 3) was generated using a droplet-based single cell platform (10X Chromium) and contains scRNA-seq data of CD11c$^+$ MHC-II$^+$ cells isolated from PBMCs of three COVID-19 patients and two HDs (**Supplementary Table 1**).

Single-cell data from datasets 1 and 3 were first visualized using non-linear dimensionality reduction through uniform manifold approximation and projection (UMAP) and graph-based clustering algorithms (**Supplementary Fig. 2A, 3A**). Clusters containing myeloid DCs were identified based on the expression of markers that discriminate cDC2s and cDC1s from all other cell populations. Specifically, *CD1C*, *FCER1A* and *CLEC10A* were used to identify cDC2s, while *CLEC9A* was used to identify cDC1s (**Supplementary Fig. 2B, 3B**). For dataset 2, myeloid DCs already annotated by the authors were considered *(23)*. Clusters recognized as myeloid DCs in the three datasets were re-clustered in further iterations to separate cDC1s from cDC2s, to discriminate cDC2 subpopulations and to exclude possible contaminants. Specifically, DC3s were distinguished from DC2s based on the expression of *CD14*, *CD163* and *S100A8* markers. This approach allowed us to clearly identify cDC subsets (**Fig. 1B and Supplementary Fig. 2C,D**).

Next, in order to unravel the transcriptional response of each DC subset during SARS-CoV-2 infection, we aggregated cell-level counts into sample-level pseudobulk counts and identified differentially expressed genes (DEGs) between COVID-19 patients and HDs (**Supplementary**

Table 2). The low numbers of cDC1s allowed their analysis only in dataset 1. In all DC subsets from the three datasets, when comparing expression profiles from COVID-19 patients with those from HDs, most of the genes up-regulated in COVID-19 were interferon (IFN) stimulated genes (ISGs) (**Fig. 1C and Supplementary Fig. 4A,B**).

To understand more deeply which biological signaling pathways were differentially regulated in COVID-19 patients compared with HDs, we performed Gene Set Enrichment Analysis (GSEA) using two different gene sets: the Hallmark collection from the Molecular Signatures Database (MSigDB) and the literature-derived Blood Transcription Modules (BTMs) (**Supplementary Table 3**) *(24)***.** As it could be predicted by the identified DEGs, in all DC subtypes from the three datasets, maturation was dominated by ISGs while we could not detect the up-regulation of inflammatory signatures containing classical activation markers and cytokines (**Fig. 1D and Supplementary Fig. 5A).** The enrichment of the inflammatory response pathway from the Hallmark collection in DC subsets of COVID-19 patients from datasets 1 and 2 (**Fig. 1D)** was due to an overlap between the genes in this pathway and those from IFN pathways. Indeed, many genes in the leading edge of the inflammatory response pathway were actually ISGs, such as *IFITM1, IRF7, LY6E* and *AXL*.

To further characterize the expression of ISGs and inflammatory molecules in DCs during SARS-CoV-2 infection, we performed a Principal Component Analysis (PCA) on the first dataset projecting single cells onto the first two principal components (PCs) (**Fig. 1E**). PC1 drives the separation between samples based on disease severity, while PC2 drives the separation between DC2 and DC3 subsets (**Fig. 1E, upper left panel and Supplementary Fig. 6A**). Patterns of ISGs and inflammatory molecules were along PC1: specifically, ISGs were highly expressed in DCs from severe COVID-19 samples, then decreased in mild COVID-19 samples and were not expressed in HDs. This is consistent with the fact that type I IFNs, although produced at similar levels in mild and severe patients early after infection, show sustained levels over time in severe patients *(2)*. Genes encoding inflammatory molecules, like *IL1B* and *CXCL8,* showed a baseline level of expression in HDs that progressively decreased with disease severity (**Fig. 1E, lower left panel**). Therefore, ISGs expression distribution showed a strong anti-correlation with that of specific inflammatory cytokines. Furthermore, analysis of the PCA loadings showed that the ISG response was orthogonal to the lineage differentiation markers of DC2s and DC3s (**Fig. 1E, right panel**), indicating that both DC2s and DC3s were equally affected by type I IFNs.

This pattern of anti-correlation between ISGs and inflammatory molecules was also evident in the second dataset analyzed (**Supplementary Fig. 6B,C,D**) and highlights again the unique ISGs response in DC subsets during SARS-CoV-2 infection.

The lack of a classical maturation signature in circulating DCs prompted us to ask whether it was possible to identify activated DCs in the blood. It could not be excluded that mature DCs reach circulation too late after activation when they are exhausted.

We, therefore, investigated the transcriptional responses of circulating DC2 and DC3 subsets in two distinct publicly available datasets: the dataset from Reyes *et al*. *(25)* containing scRNA-seq data of PBMCs and enriched DCs from patients with urinary tract bacterial infections of increasing severity (localized infection [Leuk-UTI], systemic infection with transient [Int-URO] or persistent organ dysfunctions [URO]), and the dataset from Hao *et al. (26)* containing CITE-seq data of PBMCs from healthy volunteers that received an adenovirus-based vaccine. As previously described, we performed dimensionality reduction and unsupervised clustering to identify DC subpopulations. Our approach clearly identified DC subsets in both datasets (**Fig. 2A and Supplementary Fig. 7**). We then determined DEGs in infected or vaccinated donors with respect to the corresponding HDs (**Supplementary Table 4**) and performed GSEA. The results were in stark contrast to those obtained from COVID-19 patients. Indeed, in both datasets, circulating DC2s and DC3s showed an up-regulation not only of IFN pathways (as in COVID-19) but also of inflammatory signatures and genes relevant for immune responses (differently from COVID-19) (**Fig. 2B,C and Supplementary Fig. 8,9**). Among the most highly up-regulated genes there were several encoding pro-inflammatory molecules such as *CCR1*, *CCR5*, *CXCL10*, *TNFSF10* (*CD253/TRAIL*) and *TNFSF13B* (*CD267*) as well as Toll-like receptor (TLR) genes, (**Fig. 2B and Supplementary Fig. 8A,B**).

These findings were confirmed by pathway analysis, which showed a clear activation of inflammatory pathways in DC2 and DC3 subsets in response to bacterial infections or vaccine, such as the inflammatory response pathway and the TNF-α signaling pathway (**Fig. 2C and Supplementary Fig. 9A**). Interestingly, we observed a stronger inflammatory response of circulating cDC2s in patients with localized bacterial infections (Leuk-UTI group) than in patients with bacterial sepsis (URO group). This was expected since sepsis induces functional impairment of myeloid cells, and it indicates that activated DCs can be detectable in the blood even when infections are localized, differently from COVID-19.

In addition to IFN-induced pathways, the PI3K-AKT-mTOR pathway was consistently up-regulated in all three COVID-19 datasets (**Fig. 1D**) and a down-regulation of genes encoding MHC class II molecules was also evident (**Fig. 3A).** The PI3K-AKT-mTOR pathway is

interesting in the context of SARS-CoV-2 infections since it is induced by IL-6 *(27)*, a cytokine particularly relevant in COVID-19 pathogenesis.

Therefore, COVID-19 cDCs showed three major features: i) the up-regulation of ISGs and PI3K-AKT-mTOR pathway, ii) the lack of a clear inflammatory signature, iii) the down-regulation of MHC class II molecules. We wondered whether these features could be due to the presence of mediators released during SARS-CoV-2 infection or to the direct interaction with the virus. The first cDC characteristic is compatible with both the direct interaction with the virus and the exposure to paracrine cytokines, i.e IFNs and IL-6 produced by bystander cells. By contrast, the systematic down-regulation of genes encoding MHC class II molecules is more likely explained by a direct interaction of cDCs with the virus. This prediction was also supported by evidence that the virus can infect monocyte derived DCs *(28)*.

Therefore, we investigated whether the direct interaction of cDC2s with the virus could induce a similar response to that found in the scRNA-seq datasets.

By using IL-6 and MHC class II as readouts, we measured the response to the virus of cDC2s ($CD1c^{+}CD19^{-}$ cells) freshly isolated from HDs. As predicted, we found that SARS-CoV-2 directly induced a significant down-regulation of MHC class II surface expression and the up-regulation of IL-6 in both DC2s and DC3s (**Fig. 3B,C)**. This suggests that the peculiar cDC state of maturation observed in vivo can be directly imposed by the virus as an efficient immune escape mechanism.

Data shown till now suggest that the responses of DC2s and DC3s to SARS-CoV-2 infections are very similar. Nevertheless, recent studies have indicated functional differences between DC2 and DC3 subpopulations *(29)*. In order to further investigate a potential specific role for DC3s with respect to DC2s, we determined the genes differentially induced/downmodulated by these two subpopulations in response to SARS-CoV-2 infection and bacterial sepsis.

Only 52 genes were identified as differentially expressed in DC3s compared with DC2s in COVID-19 (dataset 1), of which 33 were up-regulated and 19 were down-regulated (**Fig. 4A**). On the other hand, 203 genes were identified as differentially regulated in DC3s compared with DC2s in patients affected by intermediate urosepsis (Int-URO condition), of which 85 were up-regulated and 118 were down-regulated (**Fig. 4B**).

These findings highlight that the peculiar differences between DC2s and DC3s, which are evident in response to bacterial sepsis, are highly attenuated in response to SARS-CoV-2 infection. The diversity in the responses of DC3s and DC2s in bacterial infections could be at least partly explained by the exclusive expression of CD14 by DC3s, since CD14 is part of the receptor complex of lipopolysaccharide (LPS), a major component of the outer membrane of

Gram-negative bacteria. Interestingly, CD14 and TLR4 form also the receptor complex of calprotectin *(30)*, an inflammatory mediator highly efficiently released in COVID-19 *(1)*. The similarity of the responses of DC2s and DC3s in COVID-19 supports the hypothesis that their peculiar maturation signature is the result of a direct interaction with the virus rather than to the exposure to inflammatory mediators released during infection, otherwise the two cell types could have shown some diversification in the responses generated by the diversified expression of receptors like CD14.

Despite these differences between SARS-CoV-2 and bacterial infections, a common feature was observed for DC3s in these two clinical conditions. In both cases, genes associated with cell cycle progression *(SH3RF1, FSCN1* for COVID-19; *GAS2L3, RGCC, TCTN1* for sepsis) were specifically up-regulated in DC3s (**Fig. 4A,B**). Moreover, pathway analysis emphasized the up-regulation of the G2M checkpoint and the mitotic spindle pathways in DC3s compared with DC2s in the COVID-19 dataset (**Fig. 4C**). Also, a down-regulation in the pathway of the apoptosis was found in both datasets, although in the COVID-19 dataset the apoptosis pathway is not indicated in Figure 4C because the p-value was greater than 0.05 (p-value = 0.0503, NES = -1.3). These results suggest that DC3s may be cells proliferating during inflammatory responses or that circulating DC3s contain some proliferating progenitors that expand the DC3 population during inflammation. This is in accordance with the fact that DC3s increase in number in acute and chronic inflammatory conditions *(15)(31)*.

In conclusion, SARS-CoV-2 is detected directly by DCs and induces down-regulation of signals necessary for activation of T lymphocytes. Understanding how DCs manage SARS-CoV-2 infection will help identify ad hoc interventions to achieve optimal adaptive responses, a prerequisite for a good prognosis *(32)(21)*.

References and Notes

1. A. Silvin, N. Chapuis, G. Dunsmore, A. G. Goubet, A. Dubuisson, L. Derosa, C. Almire, C. Hénon, O. Kosmider, N. Droin, P. Rameau, C. Catelain, A. Alfaro, C. Dussiau, C. Friedrich, E. Sourdeau, N. Marin, T. A. Szwebel, D. Cantin, L. Mouthon, D. Borderie, M. Deloger, D. Bredel, S. Mouraud, D. Drubay, M. Andrieu, A. S. Lhonneur, V. Saada, A. Stoclin, C. Willekens, F. Pommeret, F. Griscelli, L. G. Ng, Z. Zhang, P. Bost, I. Amit, F. Barlesi, A. Marabelle, F. Pène, B. Gachot, F. André, L. Zitvogel, F. Ginhoux, M. Fontenay, E. Solary, Elevated Calprotectin and Abnormal Myeloid Cell Subsets Discriminate Severe from Mild COVID-19, *Cell* (2020), doi:10.1016/j.cell.2020.08.002.

2. C. Lucas, P. Wong, J. Klein, T. B. R. Castro, J. Silva, M. Sundaram, M. K. Ellingson, T. Mao, J. E. Oh, B. Israelow, T. Takahashi, M. Tokuyama, P. Lu, A. Venkataraman, A. Park, S. Mohanty, H. Wang, A. L. Wyllie, C. B. F. Vogels, R. Earnest, S. Lapidus, I. M. Ott, A. J. Moore, M. C. Muenker, J. B. Fournier, M. Campbell, C. D. Odio, A. Casanovas-Massana, A. Obaid, A. Lu-Culligan, A. Nelson, A. Brito, A. Nunez, A. Martin, A. Watkins, B. Geng, C. Kalinich, C. Harden, C. Todeasa, C. Jensen, D. Kim, D. McDonald, D. Shepard, E. Courchaine, E. B. White, E. Song, E. Silva, E. Kudo, G. DeIuliis, H. Rahming, H. J. Park, I. Matos, J. Nouws, J. Valdez, J. Fauver, J. Lim, K. A. Rose, K. Anastasio, K. Brower, L. Glick, L. Sharma, L. Sewanan, L. Knaggs, M. Minasyan, M. Batsu, M. Petrone, M. Kuang, M. Nakahata, M. Campbell, M. Linehan, M. H. Askenase, M. Simonov, M. Smolgovsky, N. Sonnert, N. Naushad, P. Vijayakumar, R. Martinello, R. Datta, R. Handoko, S. Bermejo, S. Prophet, S. Bickerton, S. Velazquez, T. Alpert, T. Rice, W. Khoury-Hanold, X. Peng, Y. Yang, Y. Cao, Y. Strong, R. Herbst, A. C. Shaw, R. Medzhitov, W. L. Schulz, N. D. Grubaugh, C. Dela Cruz, S. Farhadian, A. I. Ko, S. B. Omer, A. Iwasaki, Longitudinal analyses reveal immunological misfiring in severe COVID-19, *Nature* (2020), doi:10.1038/s41586-020-2588-y.

3. N. Mangalmurti, C. A. Hunter, Cytokine Storms: Understanding COVID-19*Immunity* (2020), doi:10.1016/j.immuni.2020.06.017.

4. J. T. Merrill, D. Erkan, J. Winakur, J. A. James, Emerging evidence of a COVID-19 thrombotic syndrome has treatment implications*Nature Reviews Rheumatology* (2020), doi:10.1038/s41584-020-0474-5.

5. Z. Wu, J. M. McGoogan, Characteristics of and Important Lessons from the Coronavirus Disease 2019 (COVID-19) Outbreak in China: Summary of a Report of 72314 Cases from the Chinese Center for Disease Control and Prevention*JAMA - Journal of the American Medical Association* (2020), doi:10.1001/jama.2020.2648.

6. A. G. Laing, A. Lorenc, I. del Molino del Barrio, A. Das, M. Fish, L. Monin, M. Muñoz-Ruiz, D. R. McKenzie, T. S. Hayday, I. Francos-Quijorna, S. Kamdar, M. Joseph, D. Davies, R. Davis, A. Jennings, I. Zlatareva, P. Vantourout, Y. Wu, V. Sofra, F. Cano, M. Greco, E. Theodoridis, J. Freedman, S. Gee, J. N. E. Chan, S. Ryan, E. Bugallo-Blanco, P. Peterson, K. Kisand, L. Haljasmägi, L. Chadli, P. Moingeon, L. Martinez, B. Merrick, K. Bisnauthsing, K. Brooks, M. A. A. Ibrahim, J. Mason, F. Lopez Gomez, K. Babalola, S. Abdul-Jawad, J. Cason, C. Mant, J. Seow, C. Graham, K. J. Doores, F. Di Rosa, J. Edgeworth, M. Shankar-Hari, A. C. Hayday, A dynamic COVID-19 immune signature includes associations with poor prognosis, *Nature Medicine* (2020), doi:10.1038/s41591-020-1038-6.

7. M. Cabeza-Cabrerizo, A. Cardoso, C. M. Minutti, M. Pereira da Costa, C. Reis e Sousa, Dendritic Cells Revisited, *Annual Review of Immunology* (2021), doi:10.1146/annurev-immunol-061020-053707.

8. S. C. Eisenbarth, Dendritic cell subsets in T cell programming: location dictates function*Nature Reviews Immunology* (2019), doi:10.1038/s41577-018-0088-1.

9. P. See, C. A. Dutertre, J. Chen, P. Günther, N. McGovern, S. E. Irac, M. Gunawan, M. Beyer, K. Händler, K. Duan, H. R. Bin Sumatoh, N. Ruffin, M. Jouve, E. Gea-Mallorquí, R. C. M. Hennekam, T. Lim, C. C. Yip, M. Wen, B. Malleret, I. Low, N. B. Shadan, C. F. S. Fen, A. Tay, J. Lum, F. Zolezzi, A. Larbi, M. Poidinger, J. K. Y. Chan, Q. Chen, L. Rénia, M. Haniffa, P. Benaroch, A. Schlitzer, J. L. Schultze, E. W. Newell, F. Ginhoux, Mapping the human DC lineage through the integration of high-dimensional techniques, *Science* (2017), doi:10.1126/science.aag3009.

10. D. A. Anderson, C. A. Dutertre, F. Ginhoux, K. M. Murphy, Genetic models of human and mouse dendritic cell development and function*Nature Reviews Immunology* (2020), doi:10.1038/s41577-020-00413-x.

11. M. Guilliams, C. A. Dutertre, C. L. Scott, N. McGovern, D. Sichien, S. Chakarov, S. Van Gassen, J. Chen, M. Poidinger, S. De Prijck, S. J. Tavernier, I. Low, S. E. Irac, C. N. Mattar, H. R. Sumatoh, G. H. L. Low, T. J. K. Chung, D. K. H. Chan, K. K. Tan, T. L. K. Hon, E. Fossum, B. Bogen, M. Choolani, J. K. Y. Chan, A. Larbi, H. Luche, S. Henri, Y. Saeys, E. W. Newell, B. N. Lambrecht, B. Malissen, F. Ginhoux, Unsupervised High-Dimensional Analysis Aligns Dendritic Cells across Tissues and Species, *Immunity* (2016), doi:10.1016/j.immuni.2016.08.015.

12. J. Canton, H. Blees, C. M. Henry, M. D. Buck, O. Schulz, N. C. Rogers, E. Childs, S. Zelenay, H. Rhys, M. C. Domart, L. Collinson, A. Alloatti, C. J. Ellison, S. Amigorena, V. Papayannopoulos, D. C. Thomas, F. Randow, C. Reis e Sousa, The receptor DNGR-1 signals for phagosomal rupture to promote cross-presentation of dead-cell-associated antigens, *Nature Immunology* (2021), doi:10.1038/s41590-020-00824-x.

13. S. L. Jongbloed, A. J. Kassianos, K. J. McDonald, G. J. Clark, X. Ju, C. E. Angel, C. J. J. Chen, P. R. Dunbar, R. B. Wadley, V. Jeet, A. J. E. Vulink, D. N. J. Hart, K. J. Radford, Human CD141+ (BDCA-3)+ dendritic cells (DCs) represent a unique myeloid DC subset that cross-presents necrotic cell antigens, *Journal of Experimental Medicine* (2010), doi:10.1084/jem.20092140.

14. G. Nizzoli, J. Krietsch, A. Weick, S. Steinfelder, F. Facciotti, P. Gruarin, A. Bianco, B. Steckel, M. Moro, M. Crosti, C. Romagnani, K. Stölzel, S. Torretta, L. Pignataro, C. Scheibenbogen, P. Neddermann, R. De Francesco, S. Abrignani, J. Geginat, Human CD1c+ dendritic cells secrete high levels of IL-12 and potently prime cytotoxic T-cell responses, *Blood* (2013), doi:10.1182/blood-2013-04-495424.

15. C. Ad. Utertre, E. Becht, S. E. Irac, A. Khalilnezhad, V. Narang, S. Khalilnezhad, P. Y. Ng, L. L. van den Hoogen, J. Y. Leong, B. Lee, M. Chevrier, X. M. Zhang, P. J. A. Yong, G. Koh, J. Lum, S. W. Howland, E. Mok, J. Chen, A. Larbi, H. K. K. Tan, T. K. H. Lim, P. Karagianni, A. G. Tzioufas, B. Malleret, J. Brody, S. Albani, J. van Roon, T. Radstake, E. W. Newell, F. Ginhoux, Single-Cell Analysis of Human Mononuclear Phagocytes Reveals Subset-Defining Markers and Identifies Circulating Inflammatory Dendritic Cells, *Immunity* (2019), doi:10.1016/j.immuni.2019.08.008.

16. A. C. Villani, R. Satija, G. Reynolds, S. Sarkizova, K. Shekhar, J. Fletcher, M. Griesbeck, A. Butler, S. Zheng, S. Lazo, L. Jardine, D. Dixon, E. Stephenson, E. Nilsson, I. Grundberg, D. McDonald, A. Filby, W. Li, P. L. De Jager, O. Rozenblatt-Rosen, A. A. Lane, M. Haniffa, A. Regev, N. Hacohen, Single-cell RNA-seq reveals new types of human blood dendritic cells, monocytes, and progenitors, *Science* (2017), doi:10.1126/science.aah4573.

17. U. Cytlak, A. Resteu, S. Pagan, K. Green, P. Milne, S. Maisuria, D. McDonald, G.

Hulme, A. Filby, B. Carpenter, R. Queen, S. Hambleton, R. Hague, H. Lango Allen, J. E. D. Thaventhiran, G. Doody, M. Collin, V. Bigley, Differential IRF8 Transcription Factor Requirement Defines Two Pathways of Dendritic Cell Development in Humans, *Immunity* (2020), doi:10.1016/j.immuni.2020.07.003.

18. I. Sánchez-Cerrillo, P. Landete, B. Aldave, S. Sánchez-Alonso, A. Sánchez-Azofra, A. Marcos-Jiménez, E. Ávalos, A. Alcaraz-Serna, I. de los Santos, T. Mateu-Albero, L. Esparcia, C. López-Sanz, P. Martínez-Fleta, L. Gabrie, L. del Campo Guerola, H. de la Fuente, M. J. Calzada, I. González-Álvaro, A. Alfranca, F. Sánchez-Madrid, C. Muñoz-Calleja, J. B. Soriano, J. Ancochea, E. Martín-Gayo, COVID-19 severity associates with pulmonary redistribution of CD1c+ DCs and inflammatory transitional and nonclassical monocytes, *Journal of Clinical Investigation* (2020), doi:10.1172/JCI140335.

19. E. Kvedaraite, L. Hertwig, I. Sinha, A. Ponzetta, I. Hed Myrberg, M. Lourda, M. Dzidic, M. Akber, J. Klingström, E. Folkesson, J. R. Muvva, P. Chen, S. Gredmark-Russ, S. Brighenti, A. Norrby-Teglund, L. I. Eriksson, O. Rooyackers, S. Aleman, K. Strålin, H.-G. Ljunggren, F. Ginhoux, N. K. Björkström, J.-I. Henter, M. Svensson, Major alterations in the mononuclear phagocyte landscape associated with COVID-19 severity, *Proceedings of the National Academy of Sciences* (2021), doi:10.1073/pnas.2018587118.

20. R. Zhou, K. K. W. To, Y. C. Wong, L. Liu, B. Zhou, X. Li, H. Huang, Y. Mo, T. Y. Luk, T. T. K. Lau, P. Yeung, W. M. Chan, A. K. L. Wu, K. C. Lung, O. T. Y. Tsang, W. S. Leung, I. F. N. Hung, K. Y. Yuen, Z. Chen, Acute SARS-CoV-2 Infection Impairs Dendritic Cell and T Cell Responses, *Immunity* (2020), doi:10.1016/j.immuni.2020.07.026.

21. A. Sette, S. Crotty, Adaptive immunity to SARS-CoV-2 and COVID-19*Cell* (2021), doi:10.1016/j.cell.2021.01.007.

22. P. S. Arunachalam, F. Wimmers, C. K. P. Mok, R. A. P. M. Perera, M. Scott, T. Hagan, N. Sigal, Y. Feng, L. Bristow, O. T. Y. Tsang, D. Wagh, J. Coller, K. L. Pellegrini, D. Kazmin, G. Alaaeddine, W. S. Leung, J. M. C. Chan, T. S. H. Chik, C. Y. C. Choi, H. CHuerta, M. P. McCullough, H. Lv, E. Anderson, S. Edupuganti, A. A. Upadhyay, S. E. Bosinger, H. Terry, P. Khatri, N. Rouphael, M. Peiris, B. Pulendran, Systems biological assessment of immunity to mild versus severe COVID-19 infection in humans, *Science* (2020), doi:10.1126/SCIENCE.ABC6261.

23. J. Schulte-Schrepping, N. Reusch, D. Paclik, K. Baßler, S. Schlickeiser, B. Zhang, B. Krämer, T. Krammer, S. Brumhard, L. Bonaguro, E. De Domenico, D. Wendisch, M. Grasshoff, T. S. Kapellos, M. Beckstette, T. Pecht, A. Saglam, O. Dietrich, H. E. Mei, A. R. Schulz, C. Conrad, D. Kunkel, E. Vafadarnejad, C. J. Xu, A. Horne, M. Herbert, A. Drews, C. Thibeault, M. Pfeiffer, S. Hippenstiel, A. Hocke, H. Müller-Redetzky, K. M. Heim, F. Machleidt, A. Uhrig, L. Bosquillon de Jarcy, L. Jürgens, M. Stegemann, C. R. Glösenkamp, H. D. Volk, C. Goffinet, M. Landthaler, E. Wyler, P. Georg, M. Schneider, C. Dang-Heine, N. Neuwinger, K. Kappert, R. Tauber, V. Corman, J. Raabe, K. M. Kaiser, M. T. Vinh, G. Rieke, C. Meisel, T. Ulas, M. Becker, R. Geffers, M. Witzenrath, C. Drosten, N. Suttorp, C. von Kalle, F. Kurth, K. Händler, J. L. Schultze, A. C. Aschenbrenner, Y. Li, J. Nattermann, B. Sawitzki, A. E. Saliba, L. E. Sander, A. Angelov, R. Bals, A. Bartholomäus, A. Becker, D. Bezdan, E. Bonifacio, P. Bork, T. Clavel, M. Colome-Tatche, A. Diefenbach, A. Dilthey, N. Fischer, K. Förstner, J. S. Frick, J. Gagneur, A. Goesmann, T. Hain, M. Hummel, S. Janssen, J. Kalinowski, R. Kallies, B. Kehr, A. Keller, S. Kim-Hellmuth, C. Klein, O. Kohlbacher, J. O. Korbel, I. Kurth, K. Ludwig, O. Makarewicz, M. Marz, A. McHardy, C. Mertes, M. Nöthen, P. Nürnberg, U. Ohler, S. Ossowski, J. Overmann, S. Peter, K. Pfeffer, A. R. Poetsch, A. Pühler, N. Rajewsky, M. Ralser, O. Rieß, S. Ripke, U. Nunes da Rocha, P. Rosenstiel, P. Schiffer, E. C. Schulte, A. Sczyrba, O. Stegle, J. Stoye, F. Theis, J. Vehreschild, J. Vogel, M. von Kleist, A. Walker, J. Walter, D. Wieczorek, J. Ziebuhr, Severe

COVID-19 Is Marked by a Dysregulated Myeloid Cell Compartment, *Cell* (2020), doi:10.1016/j.cell.2020.08.001.

24. S. Li, N. Rouphael, S. Duraisingham, S. Romero-Steiner, S. Presnell, C. Davis, D. S. Schmidt, S. E. Johnson, A. Milton, G. Rajam, S. Kasturi, G. M. Carlone, C. Quinn, D. Chaussabel, A. K. Palucka, M. J. Mulligan, R. Ahmed, D. S. Stephens, H. I. Nakaya, B. Pulendran, Molecular signatures of antibody responses derived from a systems biology study of five human vaccines, *Nature Immunology* (2014), doi:10.1038/ni.2789.

25. M. Reyes, M. R. Filbin, R. P. Bhattacharyya, K. Billman, T. Eisenhaure, D. T. Hung, B. D. Levy, R. M. Baron, P. C. Blainey, M. B. Goldberg, N. Hacohen, An immune-cell signature of bacterial sepsis*Nature Medicine* (2020), doi:10.1038/s41591-020-0752-4.

26. Y. Hao, S. Hao, E. Andersen-Nissen, W. M. Mauck, S. Zheng, A. Butler, M. J. Lee, A. J. Wilk, C. Darby, M. Zagar, P. Hoffman, M. Stoeckius, E. Papalexi, E. P. Mimitou, J. Jain, A. Srivastava, T. Stuart, L. B. Fleming, B. Yeung, A. J. Rogers, J. M. McElrath, C. A. Blish, R. Gottardo, P. Smibert, R. Satija, Integrated analysis of multimodal single-cell data*bioRxiv* (2020), doi:10.1101/2020.10.12.335331.

27. S. S. Pullamsetti, W. Seeger, R. Savai, Classical IL-6 signaling: A promising therapeutic target for pulmonary arterial hypertension*Journal of Clinical Investigation* (2018), doi:10.1172/JCI120415.

28. J. Zheng, Y. Wang, K. Li, D. K. Meyerholz, C. Allamargot, S. Perlman, Severe Acute Respiratory Syndrome Coronavirus 2–Induced Immune Activation and Death of Monocyte-Derived Human Macrophages and Dendritic Cells, *The Journal of Infectious Diseases* (2020), doi:10.1093/infdis/jiaa753.

29. P. Bourdely, G. Anselmi, K. Vaivode, R. N. Ramos, Y. Missolo-Koussou, S. Hidalgo, J. Tosselo, N. Nuñez, W. Richer, A. Vincent-Salomon, A. Saxena, K. Wood, A. Lladser, E. Piaggio, J. Helft, P. Guermonprez, Transcriptional and Functional Analysis of CD1c+ Human Dendritic Cells Identifies a CD163+ Subset Priming CD8+CD103+ T Cells, *Immunity* (2020), doi:10.1016/j.immuni.2020.06.002.

30. T. Vogl, A. Stratis, V. Wixler, T. Völler, S. Thurainayagam, S. K. Jorch, S. Zenker, A. Dreiling, D. Chakraborty, M. Fröhling, P. Paruzel, C. Wehmeyer, S. Hermann, O. Papantonopoulou, C. Geyer, K. Loser, M. Schäfers, S. Ludwig, M. Stoll, T. Leanderson, J. L. Schultze, S. König, T. Pap, J. Roth, Autoinhibitory regulation of S100A8/S100A9 alarmin activity locally restricts sterile inflammation, *Journal of Clinical Investigation* (2018), doi:10.1172/JCI89867.

31. G. Bakdash, S. I. Buschow, M. A. J. Gorris, A. Halilovic, S. V. Hato, A. E. Sköld, G. Schreibelt, S. P. Sittig, R. Torensma, T. Duiveman-De Boer, C. Schröder, E. L. Smits, C. G. Figdor, I. J. M. De Vries, Expansion of a BDCA1+ CD14+ myeloid cell population in melanoma patients may attenuate the efficacy of dendritic cell vaccines, *Cancer Research* (2016), doi:10.1158/0008-5472.CAN-15-1695.

32. A. T. Tan, M. Linster, C. W. Tan, N. Le Bert, W. N. Chia, K. Kunasegaran, Y. Zhuang, C. Y. L. Tham, A. Chia, G. J. D. Smith, B. Young, S. Kalimuddin, J. G. H. Low, D. Lye, L. F. Wang, A. Bertoletti, Early induction of functional SARS-CoV-2-specific T cells associates with rapid viral clearance and mild disease in COVID-19 patients, *Cell Reports* (2021), doi:10.1016/j.celrep.2021.108728.

Acknowledgments: RS thanks the QCB Collaboratory community directed by Matteo Pellegrini.

Funding: F.G. is supported by Fondazione Cariplo (NNATE-CoV), Fondazione Veronesi (FRACOVID), AIRC (IG 2019Id.23512), Fondazione Regionale per la Ricerca Biomedica, FRRB (IANG-CRC - CP2_12/2018), and Ministero della Salute, Ricerca Finalizzata (RF-2018-12367072).

Author contributions:
Conceptualization: FG, LM
Methodology: LM, RS, GP, VR, ARP, LS, VB, CS, MCC, SA
Investigation: LM, GP, RS, FAF, MV, FM, SA, SC, MDA, LB, AB, LN, NT
Visualization: FG, GP, LM
Funding acquisition: FG
Supervision: FG
Writing – original draft: FG, GP
Writing – review & editing: FG, GP, LM

Competing interests: RS is currently an employee of GlaxoSmithKline. The other authors declare that they have no competing interests.

Data and materials availability: All data are available in the main text or the supplementary materials.

Supplementary Materials

Materials and Methods

Figs. S1 to S9

Tables S1 to S4

References *(33-38)*

Figure legends

Fig. 1. The response of cDCs to SARS-CoV-2 infection is dominated by ISGs. (A) Percentage of cDC1s, DC2s and DC3s on $CD45^+$ cells from whole blood of COVID-19 patients (22 mild and 10 severe) and HDs (21). Statistical significance was determined using one-way analysis of variance, followed by Sidak's multiple comparison test. **p < 0.01. (B, upper panels) UMAP of cDC subtypes identified from the three scRNA-seq datasets analyzed, two publicly available (dataset 1 and dataset 2) and a newly generated one (dataset 3). Cells are colored according to cDC subtype and donor origin (lightblue, healthy controls; pink, COVID-19). (B, lower panels) Violin plots illustrating expression levels of selected marker genes used for the manual annotation of cDC subtypes. In dataset 2, cluster 7, positive for GZMB marker, was recognized as contaminant. (C) Heatmaps showing the top 100 DEGs for cDC1, DC2 and DC3 subsets comparing COVID-19 patients and HDs from dataset 1. Selected up-regulated genes (ISGs) are marked in red and down-regulated genes in blue (MHC class II). Ribosomal protein (RP) genes were removed from the top 100 DEGs. (D) GSEA of DEGs using the Hallmark collection: dataset 1 (left panel), dataset 2 (middle panel) and dataset 3 (right panel). Only pathways with a p-value < 0.05 are show. Dot size encodes the number of genes in the leading edge. NES, normalized enrichment score. (E, upper left panel) PCA from dataset 1 without Harmony correction. Cells are colored according to disease severity (grey, HDs; pink, mild COVID-19; lightblue, severe COVID-19) and DC subtype (orange, DC2; green, DC3). (E, lower left panel) Feature plots illustrating the expression distribution of selected ISGs and inflammatory molecules. (E, right panel) PCA loadings. ISGs are highlighted in red and lineage markers for DC2s and DC3s in green.

Fig. 2. Inflammatory response of cDCs during bacterial infections and adenovirus-based vaccine administration. (A) UMAP of cDC subtypes and corresponding violin plots illustrating expression levels of selected marker genes used for the manual annotation of cDC subtypes: Reyes *et al.* dataset (left panel) and Hao *et al.* dataset (right panel). (B) Heatmaps showing the top 100 DEGs for DC2 and DC3 subsets comparing: Leuk-UTI patients with HDs from Reyes *et al.* dataset (left panel) and vaccinated donors at day 3 with unvaccinated donors from Hao *et al.* dataset (right panel). Selected up-regulated genes are marked in red. Asterisk indicates genes associated with pro-inflammatory functions. Ribosomal protein (RP) genes were removed from the top 100 DEGs. (C) GSEA of DEGs using the Hallmark collection: Reyes *et al.* dataset (left panel) and Hao *et al.* dataset (right panel). Only pathways with a p-value < 0.05 are shown. Dot size encodes the number of genes in the leading edge. NES,

normalized enrichment score. Leuk-UTI, urinary tract infection with leukocytosis. Int-URO, intermediate urosepsis. URO, urosepsis.

Fig. 3. SARS-CoV-2 directly induces down-regulation of HLA-DR and production of IL-6 in DC2s and DC3s. (A) Violin plots showing the expression levels of HLA-DRA, HLA-DPB1 and HLA-DPA1 in cDC1s, DC2s and DC3s of healthy controls and COVID-19 patients from dataset 1. Healthy samples are colored in blue and COVID-19 patients in red. *$p < 0.05$, **$p < 0.01$, Wilcoxon signed-rank test. (B, upper panel) Representative histograms showing HLA-DR expression in cDC2s from HDs infected or not (NT) with 0.4 MOI of SARS-CoV-2 for 18 hours. DC2s and DC3s were identified as $CD5^+$ $CD1c^+$ and $CD5^-$ $CD1c^+$ respectively over the $CD11^+LIN^-$ (CD88, CD89, CD3 and CD19) and $Fc\varepsilon RI\alpha^+$. (B lower panel) Quantitative analysis of mean fluorescent intensity (MFI) of HLA-DR in DC2s and DC3s. Statistical significance was determined with unpaired student's t-test. *$p < 0.005$, n=4 NT and n=7 Sars-CoV-2 infected cells. (C, left panel) Representative dot plots showing the percentage of IL-6 producing DC2 and DC3 after viral infection as described in B. (C, right panel) Quantitative analysis of the percent of IL-6 producing cells. Statistical significance was determined with unpaired student's t-test. *$p < 0.005$, n=4 NT and n=7 SARS-CoV-2 infected cells.

Fig. 4. Genes differentially induced by DC2s and DC3s. Volcano plots showing genes differentially regulated in DC3s compared with DC2s in response to (A) COVID-19 (dataset 1) and (B) intermediate urosepsis (Int-URO condition, Reyes *et al.* dataset). Genes with p-value < 0.05 and absolute $\log_2$ fold change > 0.7 were considered significant. The top 10 differential genes are highlighted (red: up in DC3s; blue: up in DC2s). (C) GSEA of DEGs using the Hallmark collection: dataset 1 (left panel) and Reyes *et al*. dataset, Int-URO condition (right panel). Only pathways with a p-value < 0.05 are shown. Dot size encodes the number of genes in the leading edge. NES, normalized enrichment score.

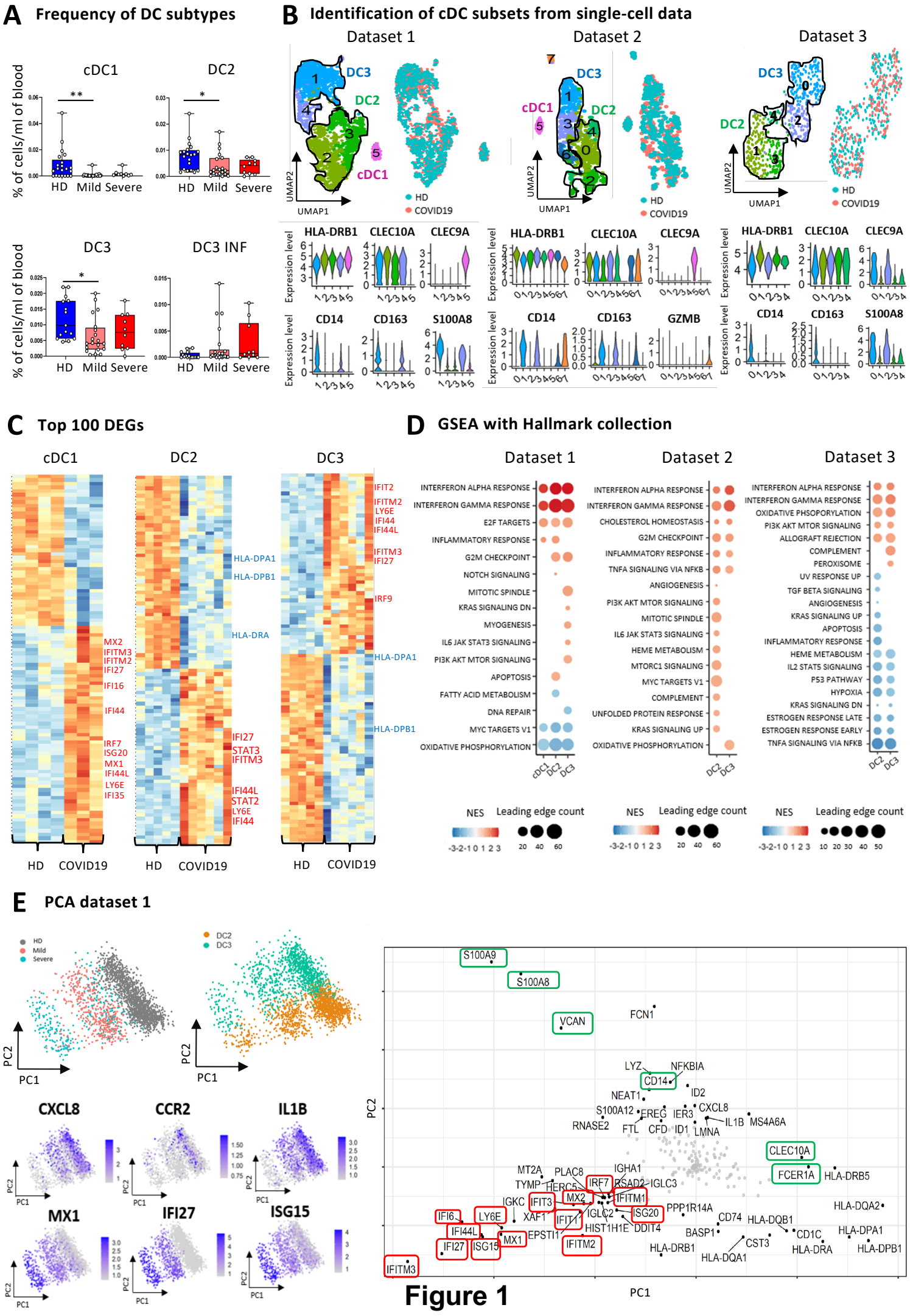
A Frequency of DC subtypes
cDC1
DC2
DC3
DC3 INF
% of cells/ml of blood
HD
Mild
Severe
B Identification of cDC subsets from single-cell data
Dataset 1
Dataset 2
Dataset 3
DC3
DC2
cDC1
UMAP1
UMAP2
HD
COVID19
HLA-DRB1
CLEC10A
CLEC9A
CD14
CD163
S100A8
GZMB
Expression level
C Top 100 DEGs
cDC1
DC2
DC3
HD
COVID19
MX2
IFITM3
IFITM2
IFI27
IFI16
IFI44
IRF7
ISG20
MX1
IFI44L
LY6E
IFI35
HLA-DPA1
HLA-DPB1
HLA-DRA
IFI27
STAT3
IFITM3
IFI44L
STAT2
LY6E
IFI44
IFIT2
IFITM2
LY6E
IFI44
IFI44L
IFITM3
IFI27
IRF9
HLA-DPA1
HLA-DPB1
D GSEA with Hallmark collection
Dataset 1
Dataset 2
Dataset 3
INTERFERON ALPHA RESPONSE
INTERFERON GAMMA RESPONSE
E2F TARGETS
INFLAMMATORY RESPONSE
G2M CHECKPOINT
NOTCH SIGNALING
MITOTIC SPINDLE
KRAS SIGNALING DN
MYOGENESIS
IL6 JAK STAT3 SIGNALING
PI3K AKT MTOR SIGNALING
APOPTOSIS
FATTY ACID METABOLISM
DNA REPAIR
MYC TARGETS V1
OXIDATIVE PHOSPHORYLATION
CHOLESTEROL HOMEOSTASIS
TNFA SIGNALING VIA NFKB
ANGIOGENESIS
HEME METABOLISM
MTORC1 SIGNALING
MYC TARGETS V1
COMPLEMENT
UNFOLDED PROTEIN RESPONSE
KRAS SIGNALING UP
OXIDATIVE PHOSPHORYLATION
ALLOGRAFT REJECTION
PEROXISOME
UV RESPONSE UP
TGF BETA SIGNALING
ESTROGEN RESPONSE LATE
ESTROGEN RESPONSE EARLY
P53 PATHWAY
HYPOXIA
NES
Leading edge count
E PCA dataset 1
HD
Mild
Severe
DC2
DC3
PC1
PC2
CXCL8
CCR2
IL1B
MX1
IFI27
ISG15
S100A9
S100A8
VCAN
FCN1
LYZ
NFKBIA
CD14
NEAT1
ID2
S100A12
EREG
IER3
CXCL8
RNASE2
FTL
CFD
ID1
IL1B
MS4A6A
LMNA
CLEC10A
FCER1A
HLA-DRB5
MT2A
PLAC8
IGHA1
TYMP
HERC5
IRF7
RSAD2
IGLC3
IGKC
IFIT3
MX2
IFITM1
IFI6
LY6E
XAF1
IFIT1
IGLC2
ISG20
PPP1R14A
HLA-DQA2
IFI44L
EPSTI1
HIST1H1E
DDIT4
CD74
HLA-DQB1
IFI27
ISG15
MX1
IFITM2
BASP1
CST3
CD1C
HLA-DPA1
HLA-DRB1
HLA-DRA
HLA-DPB1
HLA-DQA1
IFITM3

Figure 1

A Identification of cDC subsets from single-cell data

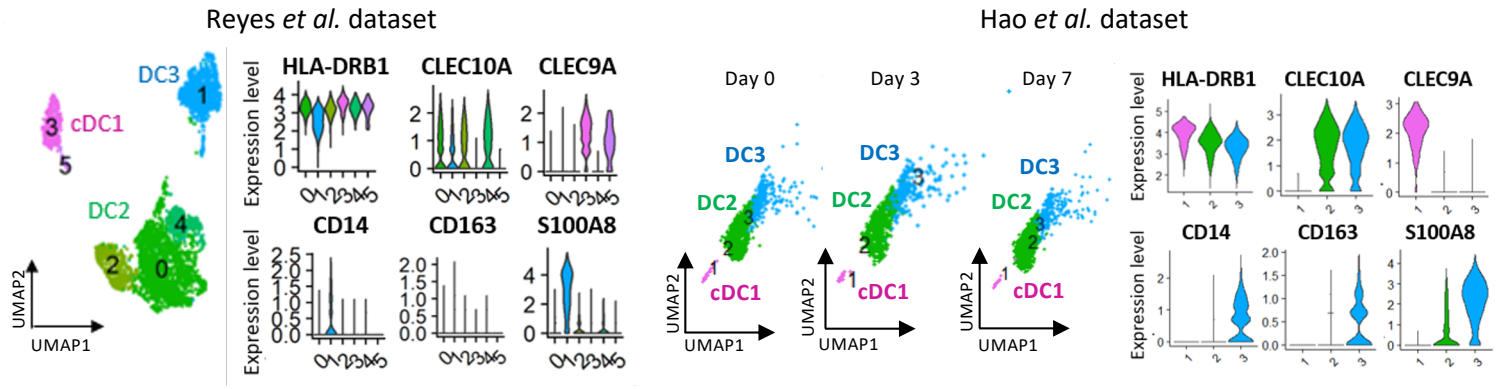

B Top 100 DEGs

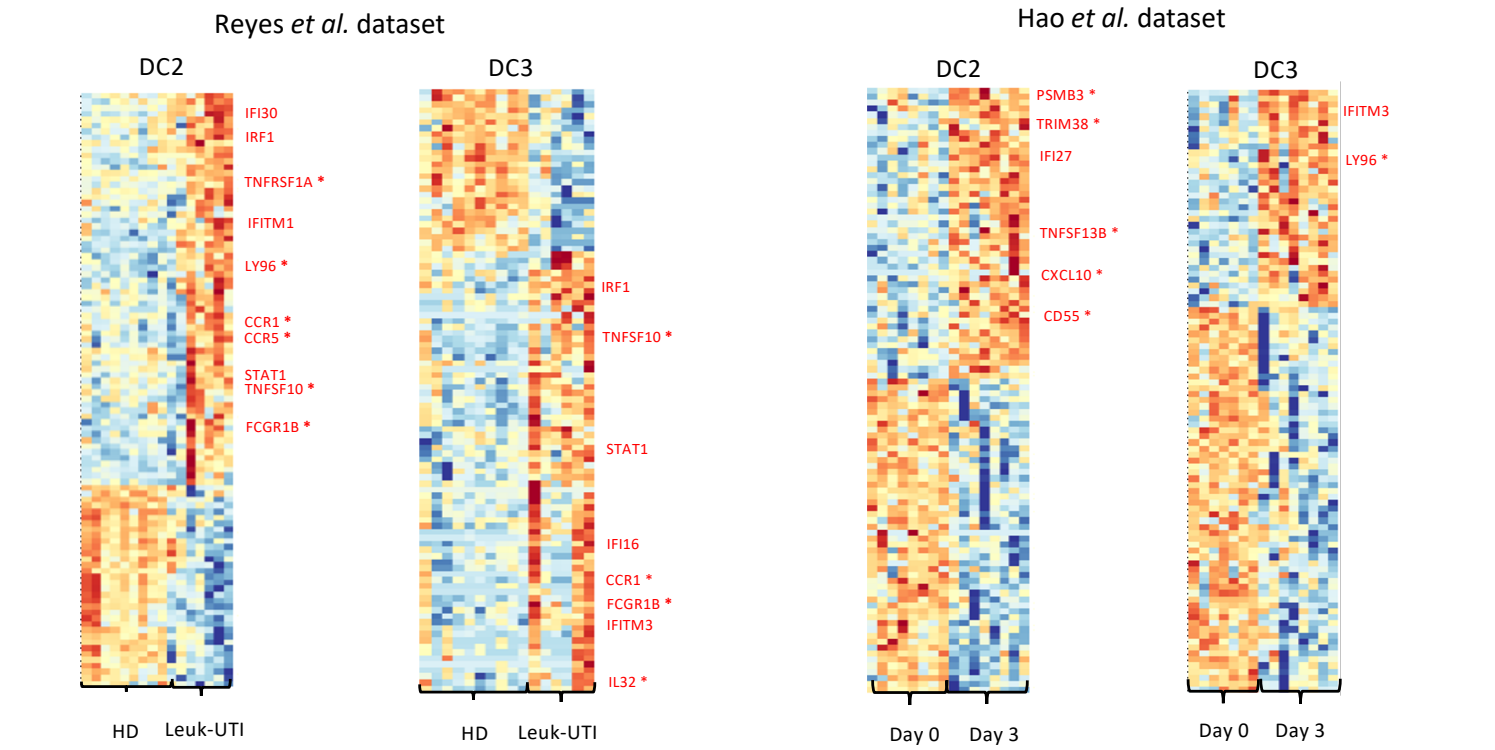

C GSEA with Hallmark collection

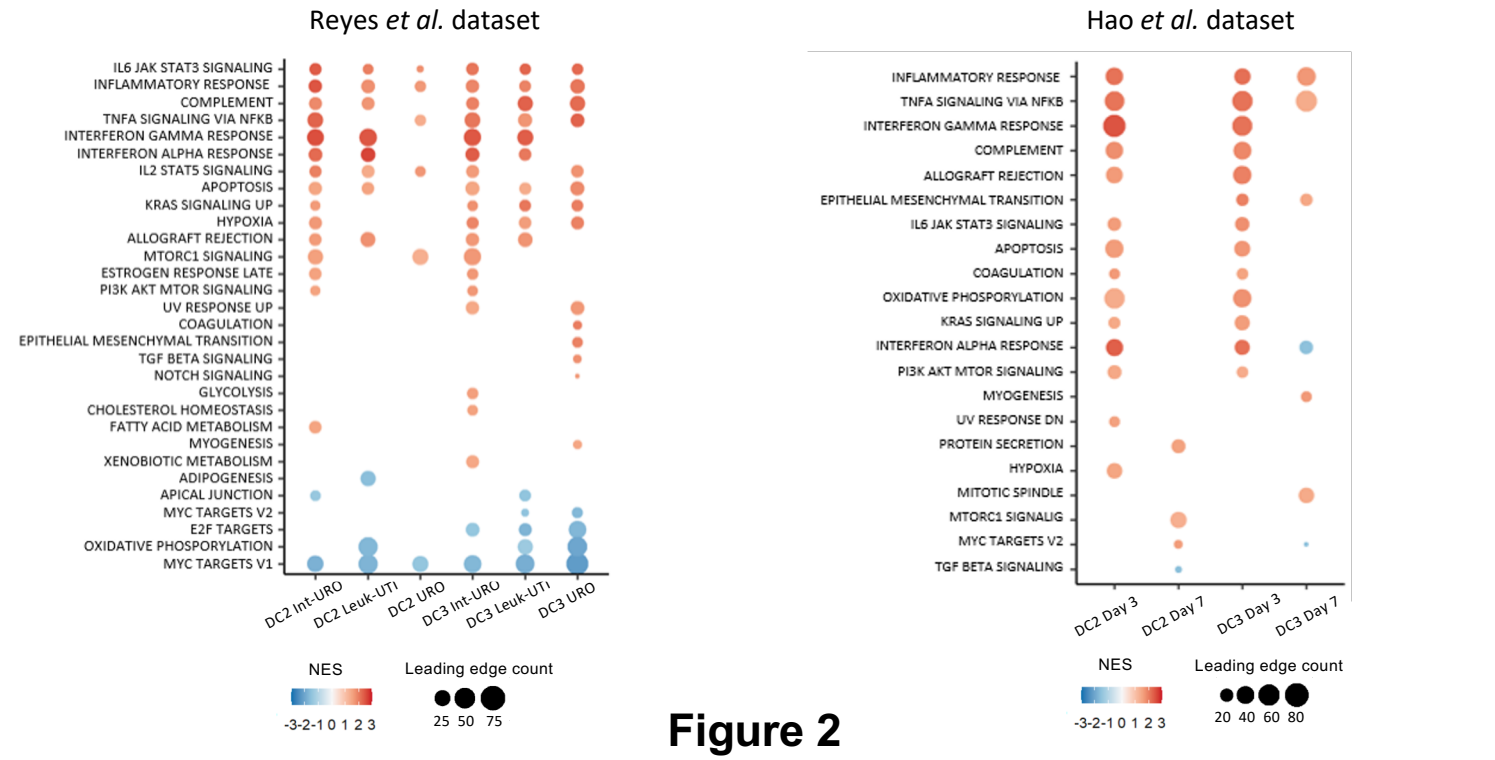

Figure 2

A Down-regulation of MHC class II genes

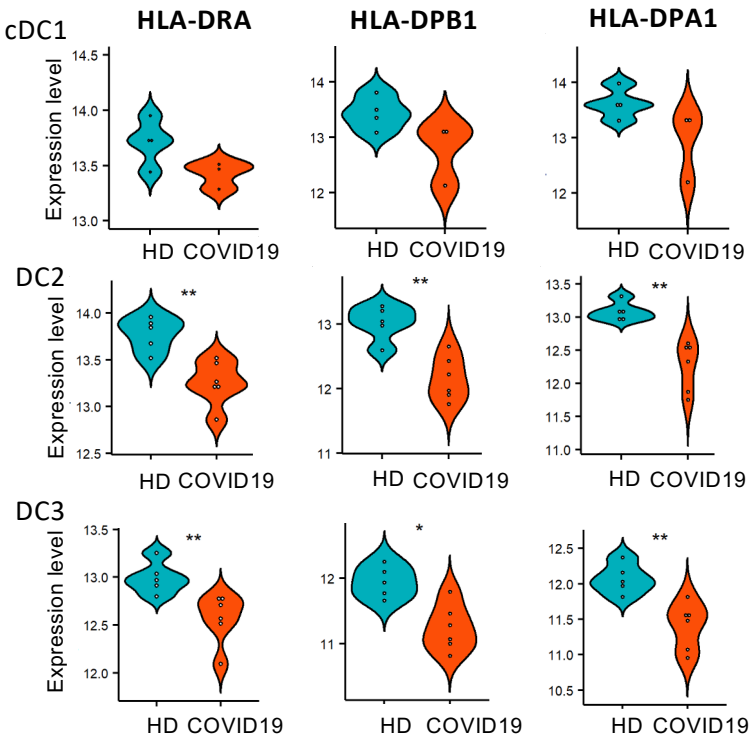

B HLA-DR expression in SARS-CoV-2 infected DC2s and DC3s

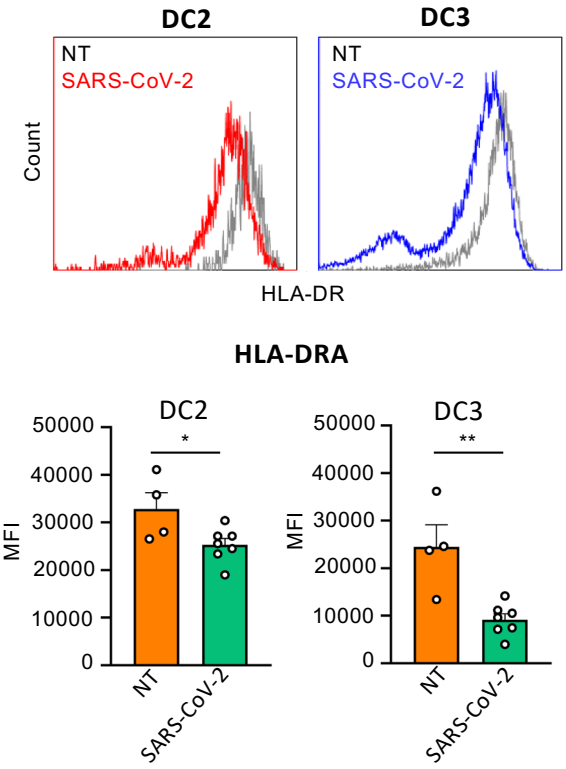

C IL-6 production from SARS-CoV-2 infected DC2s and DC3s

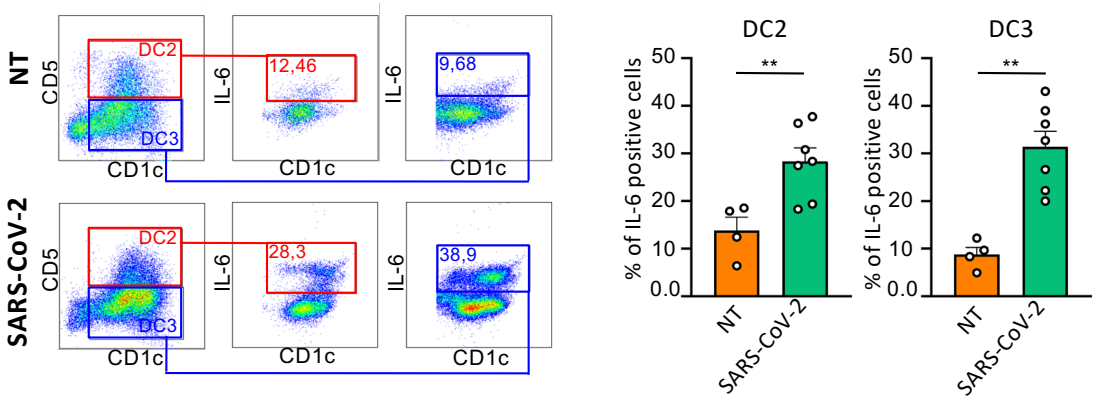

Figure 3

A **Genes differentially induced between DC3s and DC2s in response to COVID-19 (dataset 1)**

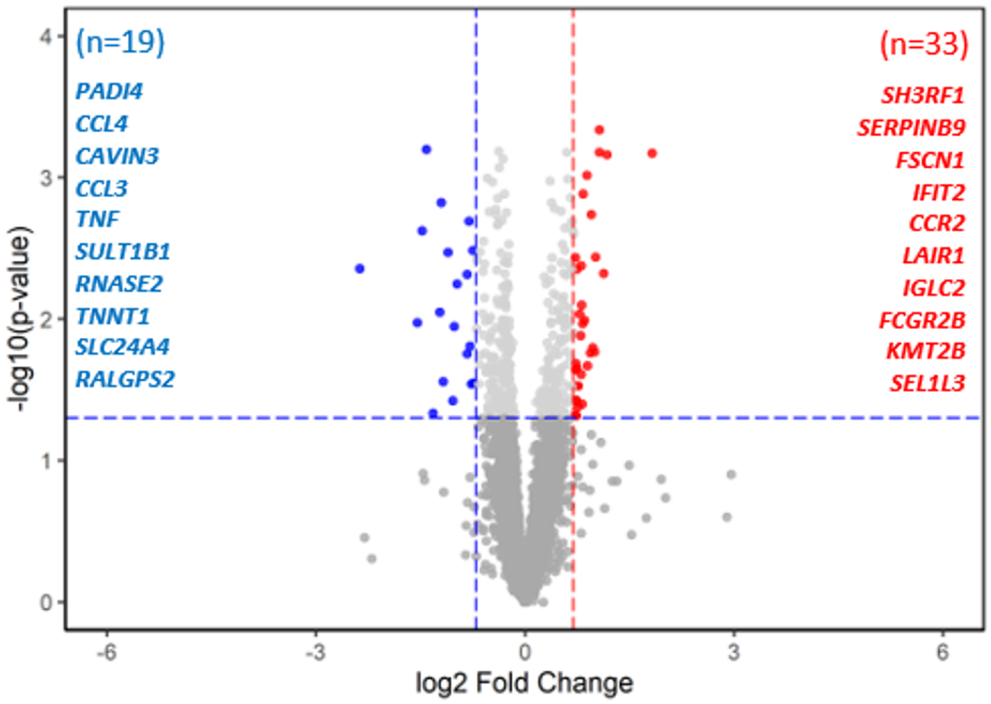

B **Genes differentially induced between DC3s and DC2s in response to bacterial infection (Int-URO condition)**

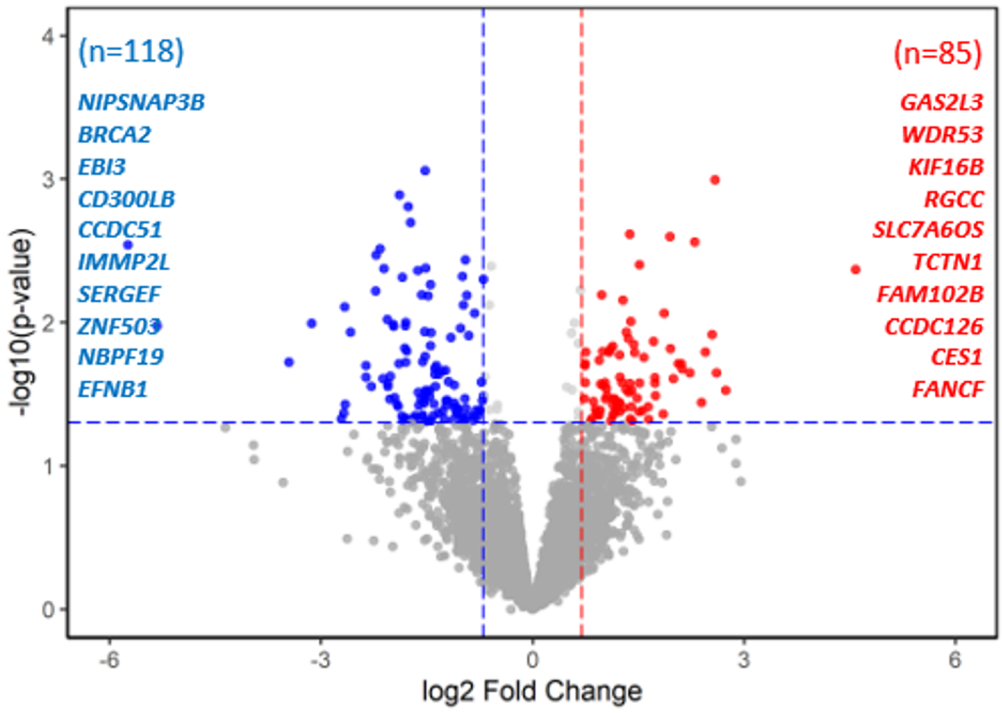

C **GSEA with Hallmark collection**

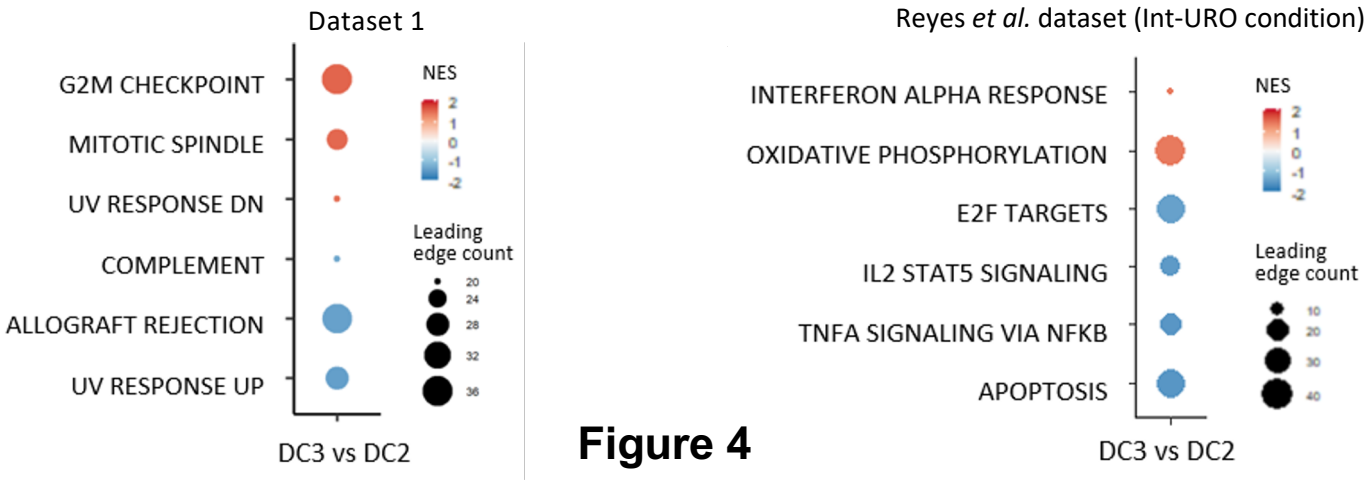

Figure 4

Maturation signatures of conventional dendritic cells in COVID-19 reflect direct viral sensing

Laura Marongiu[1,2], Giulia Protti[1,2], Fabio A. Facchini[1], Mihai Valache[1], Francesca Mingozzi[1], Valeria Ranzani[2], Anna Rita Putignano[2], Lorenzo Salviati[1,2], Valeria Bevilacqua [2], Serena Curti[2], Mariacristina Crosti[2], Mariella D'Angiò[3], Laura Rachele Bettini[3], Andrea Biondi[3], Luca Nespoli[4], Nicolò Tamini[4], Nicasio Mancini[5,6], Nicola Clementi[5,6], Sergio Abrignani[2,7], Roberto Spreafico[8], Francesca Granucci[1,2,*]

[1]Department of Biotechnology and Biosciences, University of Milano-Bicocca, Milan, Italy
[2]National Institute of Molecular Genetics "Romeo ed Enrica Invernizzi", Milan, Italy
[3]Pediatric Department and Centro Tettamanti-European Reference Network PaedCan, EuroBloodNet, MetabERN-University of Milano-Bicocca-Fondazione MBBM-Ospedale, San Gerardo, Monza, Italy.
[4]ASST san Gerardo Hospital, Monza, Italy, School of Medicine and Surgery, University of Milano-Bicocca
[5]Laboratory of Medical Microbiology and Virology, Vita-Salute San Raffaele University, Milan, Italy.
[6]IRCCS San Raffaele Hospital, Milan, Italy.
[7]Department of Clinical Sciences and Community Health, University of Milano, Milan, Italy
[8]Institute for Quantitative and Computational Biosciences, University of California, Los Angeles

Correspondence to: francesca.granucci@unimib.it; granucci@ingm.org

This PDF file includes:

Materials and Methods
Figs. S1 to S9
Tables S1 to S4
References *(33-38)*

Materials and Methods

Flow cytometric analysis

PBMCs from COVID-19 patients enrolled from the STORM cohort were extracted from peripheral blood by density gradient centrifugation using Ficoll (GE Healthcare). Cells were washed twice and stained for 30 minutes on ice using the following anti-human antibodies (1:200, Becton Dickinson): anti-FcεRIα PE-Cy7, anti-CD14 PE, anti-CD1c APC-Cy7, anti-Clec9 (CD370) Alexa 647, anti-CD5 BV786, anti-CD3 BV605, anti-CD19 BV605, anti-CD88 BV605, anti-CD89 BV605, anti-CD11c BV480, anti-CD163 BV421, anti-HLA-DR BUV805. Cells were then washed and fixed using fixation buffer (Becton Dickinson) and acquired using BD FACSsymphony instrument (Becton Dickinson). Analyses were performed with Flow jo X software**.**

cDC2s purification and activation

Human cDC2 cells were purified from peripheral blood mononuclear cells (PBMCs) extracts from buffy coat of healthy donors (provided by Niguarda hospital blood bank) by Ficoll-Paque density gradient centrifugation. Briefly, blood was stratified on Ficoll-Paque PLUS (GE Healthcare) in 3:4 ratio and centrifuged at 1500 r.p.m. for 30 min without brake. PBMCs were washed twice, collected and $CD1c^+$ cells were purified using MACS beads according to the manufacturer's instructions (Miltenyi Biotec). Cells were cultured in Roswell Park Memorial Institute (RPMI) 1640 medium (Euroclone) containing 10% heat-inactivated fetal bovine serum (Euroclone), 100 IU of penicillin, streptomycin (100 µg/ml), 2 mM l-glutamine (Euroclone). cDC2s were infected with 0.4 MOI of SARS-CoV-2 for 18h, then collected and stained with anti-FcεRIα PE-Cy7, anti-CD14 PE, anti-CD1c APC-Cy7, anti-CD5 BV786, anti-CD3 BV605, anti-CD19 BV605, anti-CD88 BV605, anti-CD89 BV605, anti-CD11c BV480, anti-CD163 BV421, anti-HLA-DR BUV805 (1:200, all from Becton Dickinson). Cells were then fixed and permeabilized with cytofix/cytoperm reagent kit (Becton Dickinson) and stained with anti-IL-6 FITC antibody, according to the manufacturer's instructions. Samples were acquired with the BD FACSsymphony instrument (Becton Dickinson) and analyzed with Kaluza software.

Single-cell RNA sequencing datasets analyzed in the study

In this study, three different scRNA-seq datasets from COVID-19 patients and healthy controls were analyzed.

Dataset 1 *(22)* is a CITE-seq experiment with PBMCs and enriched DCs from 7 COVID-19 patients and 5 HDs. Count matrices were downloaded from the Gene Expression Omnibus (GEO) (GSE155673).

Dataset 2 *(23)* is a scRNA-seq experiment with PBMCs from 18 COVID-19 patients and 21 HDs. Seurat *(26)* objects were downloaded from FASTGenomics (https://www.fastgenomics.org/). Only cells annotated as myeloid DCs by the authors were used in downstream analyses.

Dataset 3 was newly generated. Myeloid cells were sorted ($CD11c^+$ $MHCII^+$) from 3 COVID-19 patients (enrolled from the STORM cohort) and 2 healthy donors using a MACSQuant Tyto (Miltenyi) (**Supplementary Fig. 1B**). After sorting, cell number and viability were evaluated using an automated cell counter. Viability for each sample was ≥75%. 10,000 cells per sample were loaded on a Chromium Next GEM Chip G (10x Genomics). A Chromium controller (10x Genomics, Pleasanton, CA, USA) was used to generate single-cell GEMs, according to Chromium Next GEM Single Cell 5' Library & Gel Bead Kit v1.1 protocol (PN-1000165; 10x Genomics). Full-length cDNA amplification and 5' gene expression library construction were performed according to manufacturers' instructions in a Veriti 96-well Thermal Cycler (Thermo Fisher Scientific). Indexed libraries were sequenced on an Illumina Novaseq 6000 platform, on a S2 flowcell, 150bp PE (20,000 read pairs per cell). Reads from FASTQ files were aligned against the GRCh38 human reference genome and quantified using the Cell Ranger pipeline (10x Genomics) with default parameters. Single cell data have been deposited in GEO, the accession number will be published after GEO notification.

To compare transcriptional responses of cDC subsets between SARS-CoV-2 infection and other inflammatory conditions, we analyzed two additional publicly available datasets.

The Reyes *et al*. dataset *(25)* is a scRNA-seq experiment with PBMCs and enriched DCs from patients with bacterial infections and healthy controls. Briefly, subjects were enrolled in two different cohorts. A primary cohort contains subjects that were classified into three clinical categories: Leuk-UTI, Int-URO and URO. The Leuk-UTI group refers to subjects with urinary-tract infection (UTI) with leukocytosis (blood WBC ≥ 12,000 per mm^3) but no organ dysfunction. The Int-URO (intermediate urosepsis) group contains subjects with UTI with mild or transient organ dysfunction, and the URO (urosepsis) group refers to subjects with UTI with clear or persistent organ dysfunction. Ten subjects were classified as Leuk-UTI, seven as Int-URO and ten as URO. A second cohort comprises hospitalized subjects classified into three conditions: subjects with bacteremia and sepsis not requiring intensive care unit (ICU) admission (Bac-SEP group, four subjects), subjects with sepsis requiring ICU care (ICU-SEP,

eight subjects) and subjects in the ICU for conditions other than sepsis (ICU-NoSEP, seven subjects). Data were downloaded from the Broad Institute Single Cell Portal (https://singlecell.broadinstitute.org/single_cell) (SCP548). For downstream analysis, we retained monocytes and DCs as annotated by the authors.

The Hao *et al.* dataset *(26)* is a CITE-seq experiment with PBMCs from 8 healthy volunteers enrolled in an adenovirus-based HIV vaccine trial. For each subject, PBMCs were collected at three time points: immediately before (day 0), three days, and seven days following vaccine administration. Data were downloaded from https://atlas.fredhutch.org/nygc/multimodal-pbmc/. For downstream analysis, we retained only cDCs as annotated by the authors.

Single-cell data processing and analysis

Data processing and analysis for all single-cell datasets was performed using the Seurat package (version 4.0) *(26)* in R (version 4.0.3).

First, filters were applied to remove low-quality cells. These were based on the number of genes and UMIs detected in each cell and on the percentage of reads mapping to mitochondrial genes. Counts were then normalized and log-transformed using sctransform *(33)*, while regressing out UMI counts and percentage of mitochondrial counts.

For dimensionality reduction, PCA was performed. Principal components (PCs) were fed to Harmony *(34)* for batch correction and/or integration of datasets from both disease and healthy conditions. UMAP was used for 2D visualization. Clusters were identified with the shared nearest neighbour (SNN) modularity optimization-based clustering algorithm followed by Louvain or Leiden (check code) community detection. Cell type assignment was manually performed using marker genes, as detailed in figures. cDCs were retained and re-clustered again to identify subsets.

Pseudobulk differential gene expression analysis

After the identification of cDC subsets, we aggregated cell-level counts into sample-level pseudobulk counts. For each DC subset, only donors with at least 10 cells were retained.

For the dataset from Reyes *et al.*, only samples from the primary cohort were considered for differential analysis due to the low number of DCs obtained from subjects from the secondary cohort.

Differential expression analysis was performed using the quasi-likelihood framework of the edgeR package *(35)*, using each donor as the unit of independent replication.

Gene Set Enrichment Analysis

Pre-ranked GSEA *(36)* was performed on the differentially expressed genes (DEGs) using the fgsea package *(37)*. The Hallmark gene sets *(38)* and the Blood Transcription Modules (BTM) *(24)* were used. BTM families analyzed in this study are reported in Supplementary Table 3.

Code availability

Code used for data analysis will be made available upon publication.

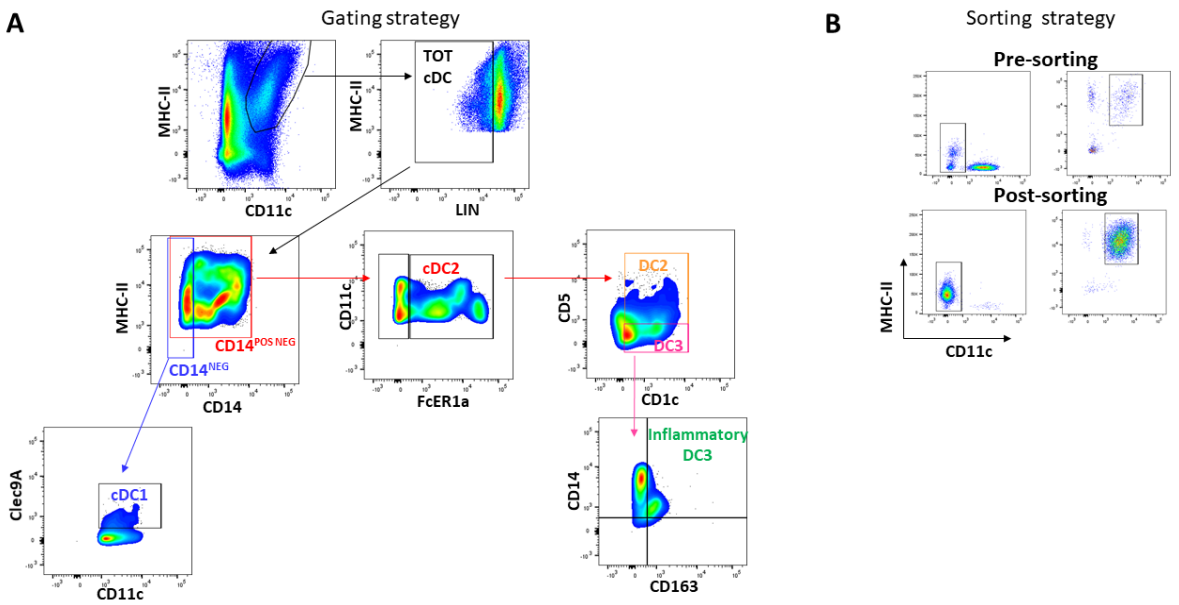

Supplementary Figure 1.

(A) Gating strategy to identify DCs subsets from PBMCs. Total DCs (cDCs TOT) were detected among the CD11c^{+} MHC-II^{+} and LIN^{-} (CD88, CD89, CD3 and CD19) population. cDC1s were identified as CLEC9A^{+} from the CD14^{-} fraction of total DCs. cDC2s (FcεRIα^{+}) include CD14^{+} and CD14^{-} cells. DC2s and DC3s were identified as CD5^{+} CD1c^{+} and CD5^{-} CD1c^{+} respectively. Inflammatory DC3s were recognized as CD14^{+}CD163^{+} cells.

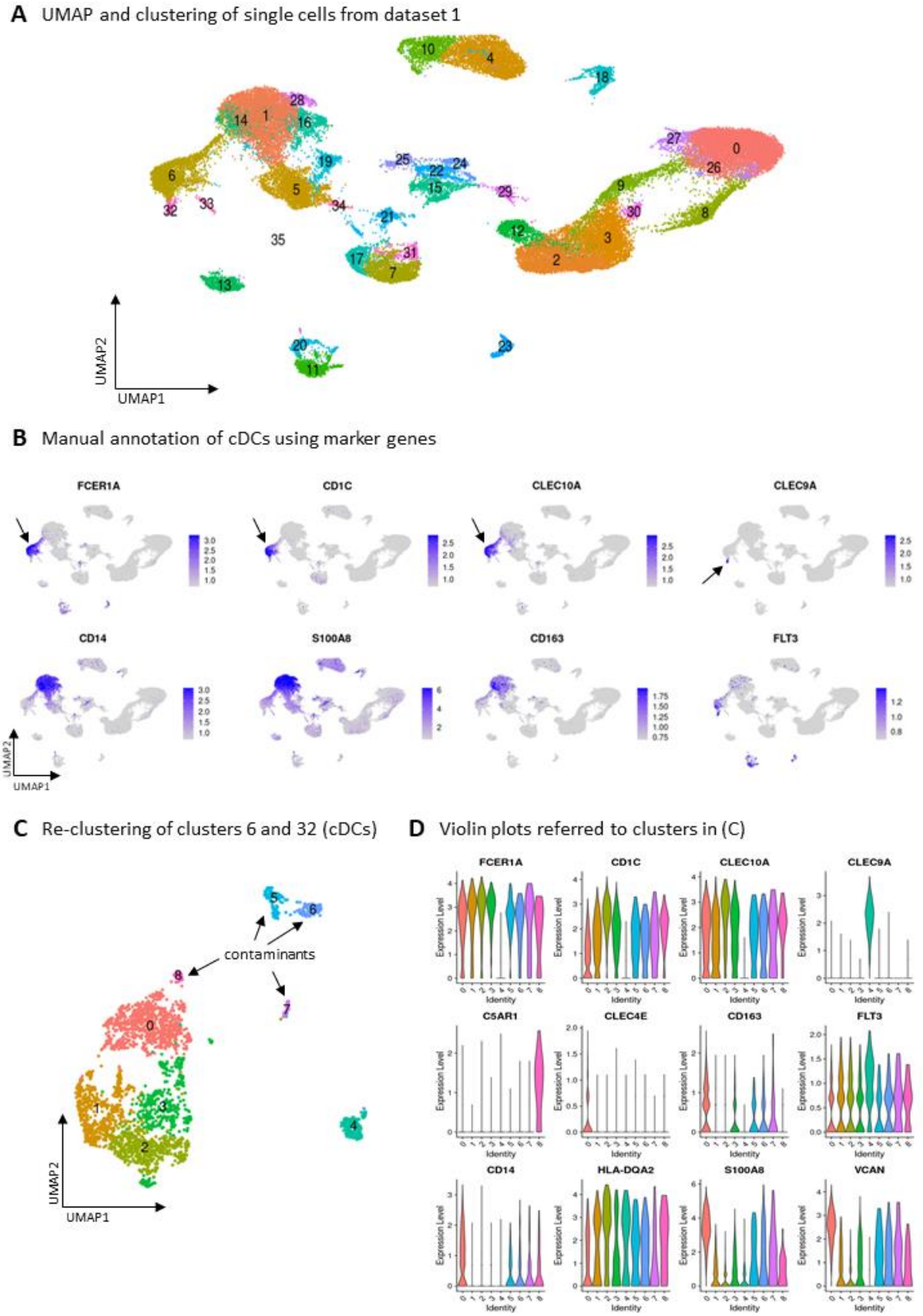

Supplementary Figure 2. Identification of cDC subpopulations in dataset 1. (A) UMAP and clustering of single cells. (B) Feature plots showing the expression levels of selected

marker genes used to identify cDC clusters. Black arrows indicate cDC clusters (cluster 6 is cDC2 and cluster 32 is cDC1). (C) Re-clustering of clusters 6 and 32 corresponding to cDCs. Clusters 5, 6, 7 and 8 were identified as contaminants. Clusters 0, 1, 2, 3 and 4 were re-clustered in a final iteration to clearly delineate cDC1, DC2 and DC3 subsets as shown in Figure 1B. (D) Violin plots referred to clusters in (C) showing expression levels of selected marker genes used to identify cDC subpopulations.

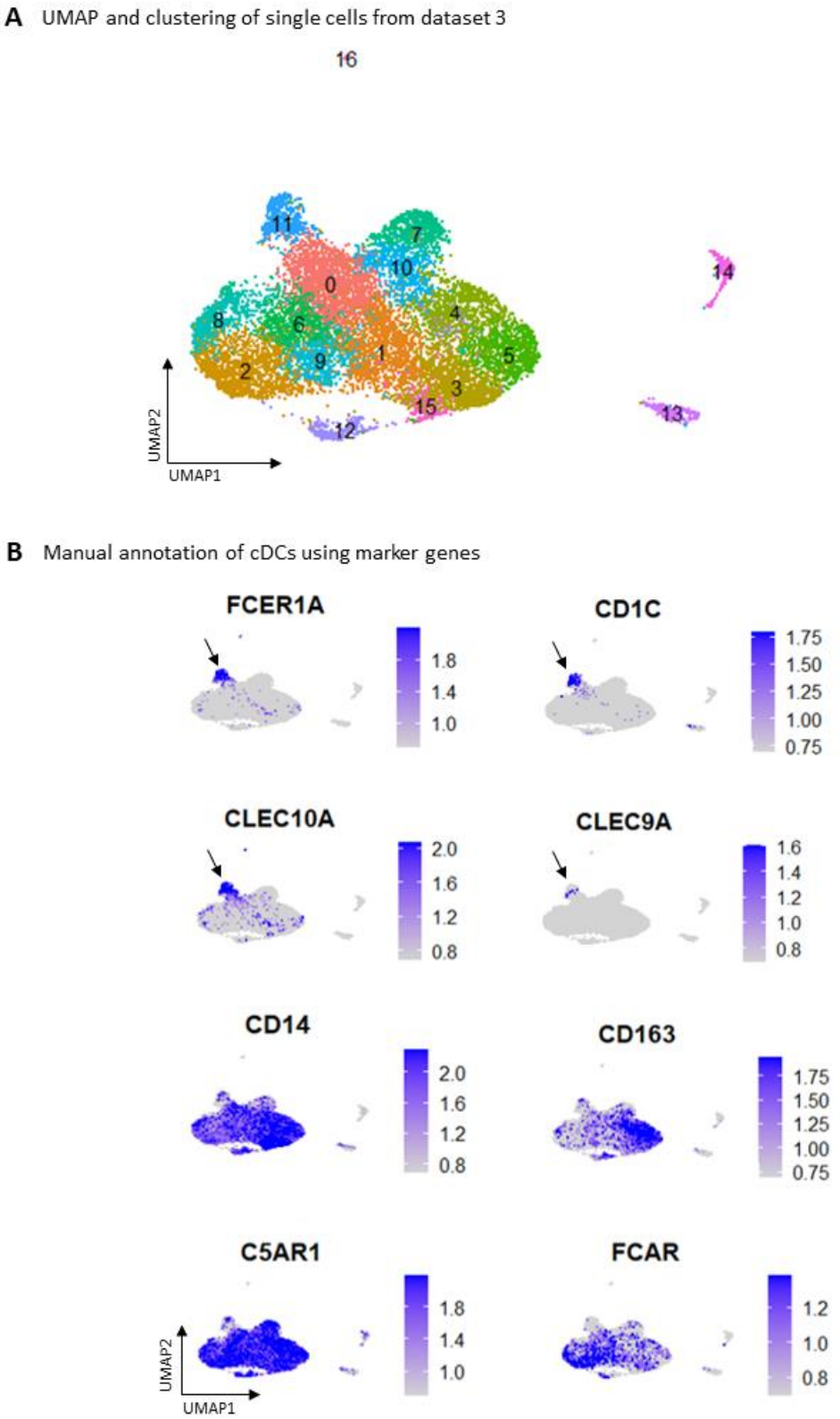

Supplementary Figure 3. Identification of cDC subpopulations in dataset 3. (A) UMAP and clustering of single cells. (B) Feature plots showing the expression levels of selected marker genes used to identify cDC cluster. Black arrows indicate cDC cluster (cluster 11). This cluster was re-clustered in a final iteration to clearly delineate cDC subsets as shown in Figure 1B.

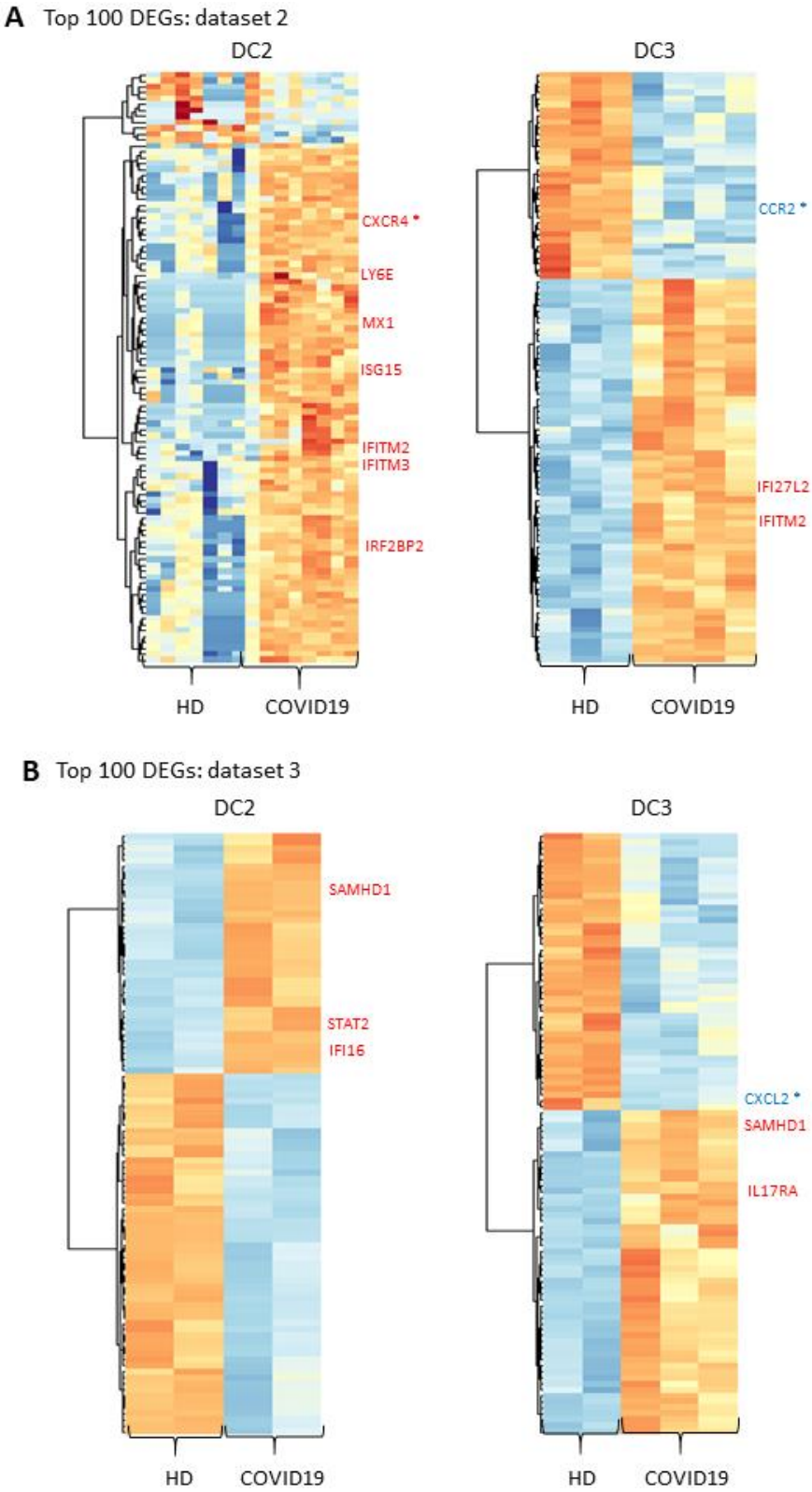

Supplementary Figure 4. Expression heatmaps showing the top 100 DEGs from datasets 2 ad 3. Heatmap showing the top 100 DEGs for DC2 and DC3 subsets comparing COVID-19 patients and HDs from (A) dataset 2 and (B) dataset 3. Selected up-regulated genes are marked in red (mainly ISGs) and down-regulated genes in blue. Asterisk indicates genes associated

with pro-inflammatory functions. Ribosomal protein (RP) genes were removed from the top 100 DEGs.

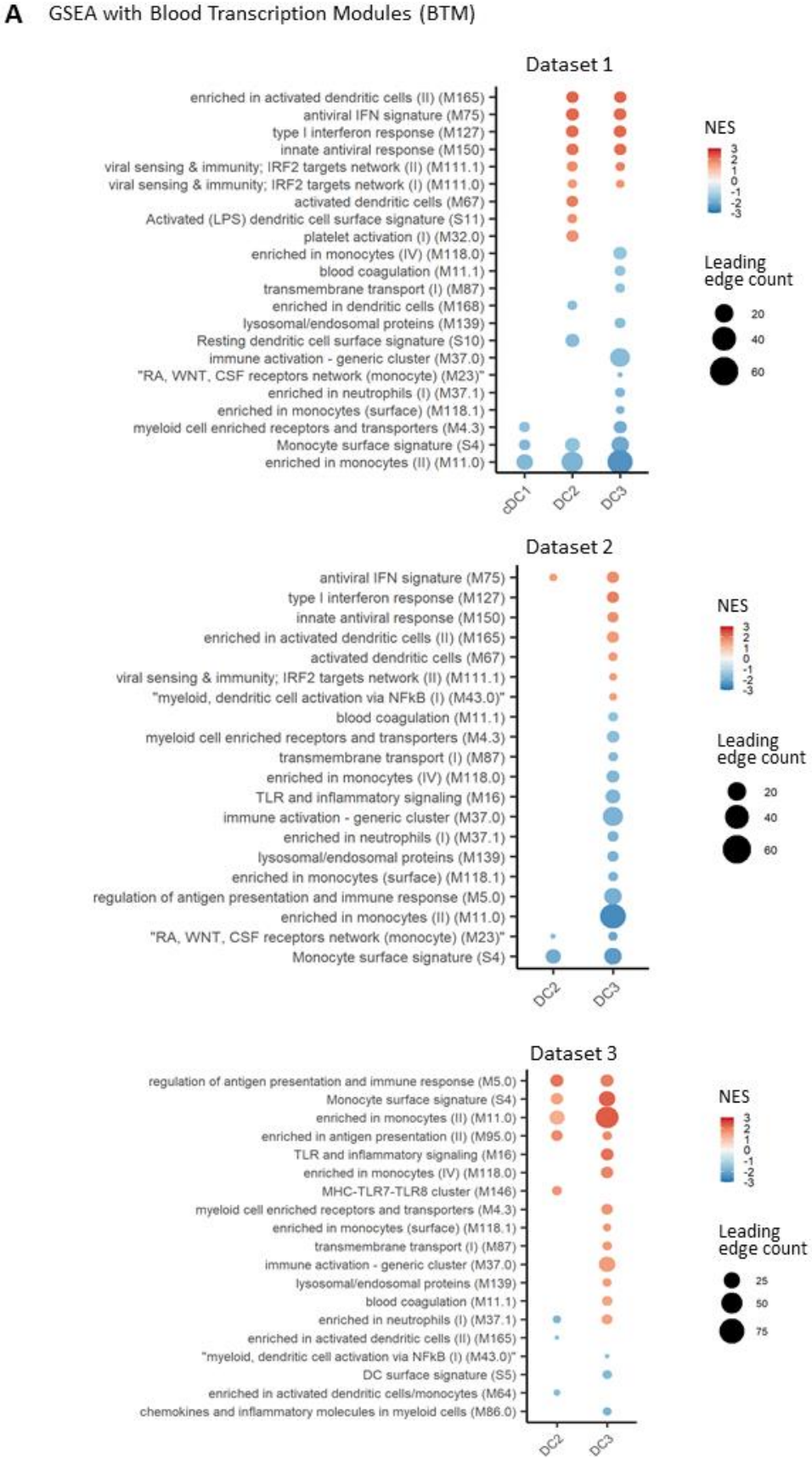

Supplementary Figure 5. GSEA with Blood Transcription Modules (BTM) for datasets 1, 2 and 3. (A) GSEA of DEGs using the BTM collection: dataset 1 (upper panel), dataset 2

(middle panel) and dataset 3 (lower panel). Only pathways with a p-value < 0.05 are shown. Dot size encodes the number of genes in the leading edge. NES, normalized enrichment score.

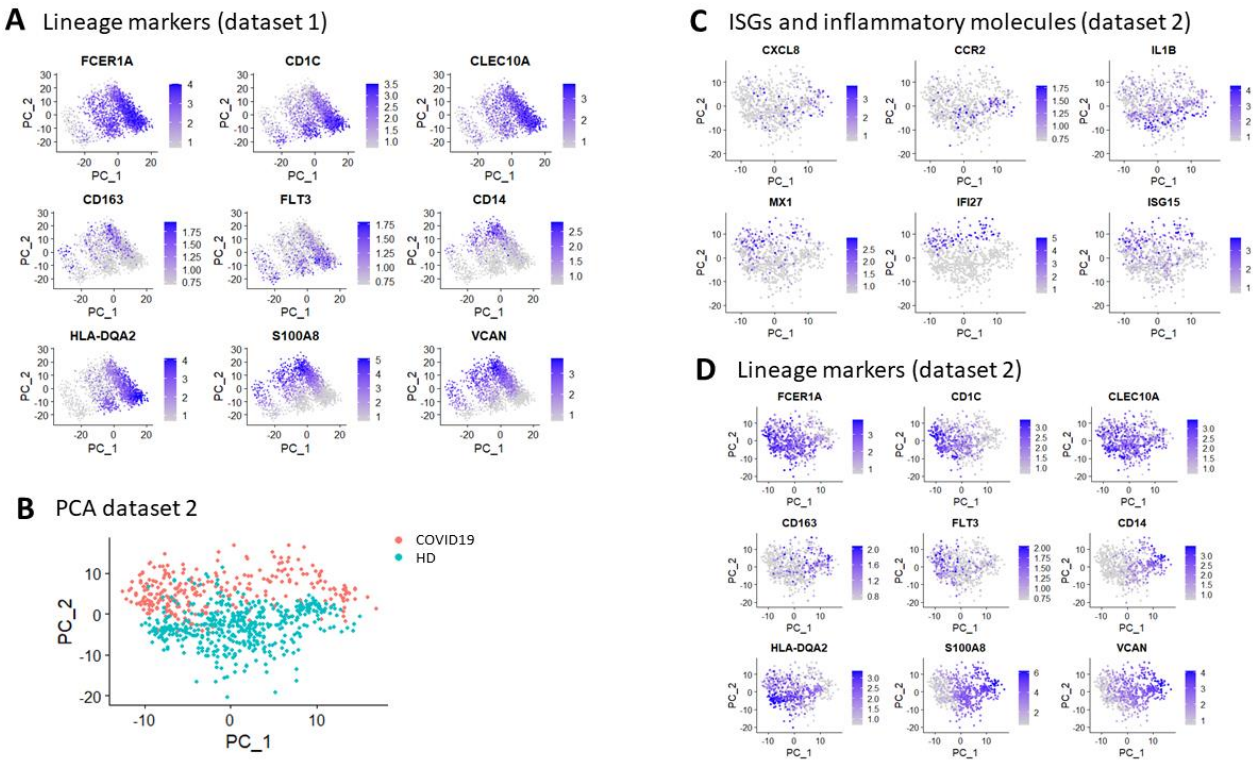

Supplementary Figure 6. PCA without Harmony correction. (A) Feature plots illustrating the expression distribution of lineage markers in dataset 1. PC2 drives the separation between DC2 and DC3 subsets. (B) PCA from dataset 2. Cells are colored according to donor origin (pink, COVID-19; lightblue, healthy controls). PC2 drives the separation between healthy and COVID-19 samples. (C) Feature plots illustrating the expression distribution of selected ISGs and inflammatory molecules. (D) Feature plots illustrating the expression distribution of lineage markers. PC1 drives the separation between DC2 and DC3 subsets.

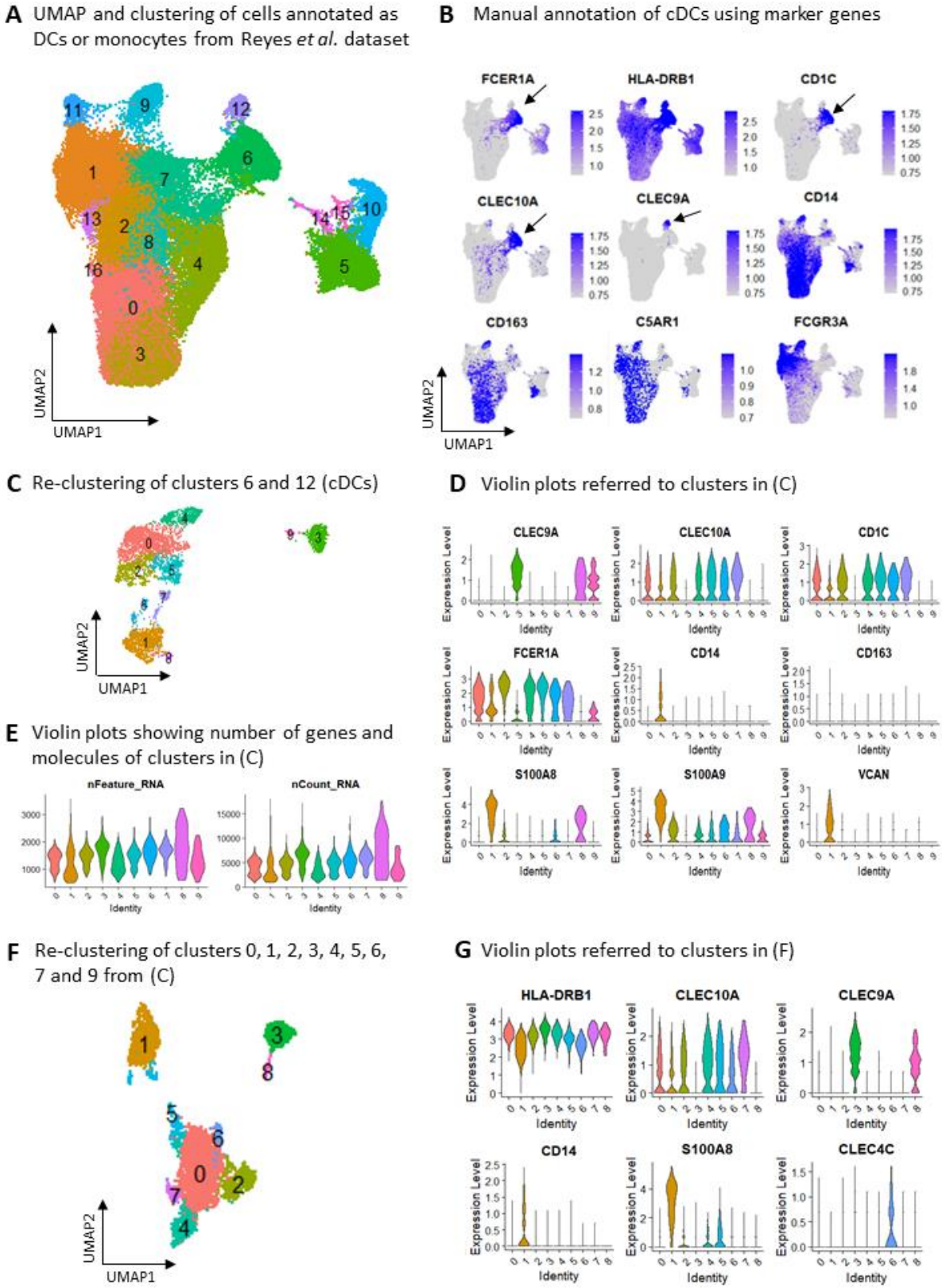

Supplementary Figure 7. Identification of cDC subpopulations in the dataset from Reyes *et al.* (A) UMAP and clustering of cells annotated as DCs or monocytes by the authors. (B) Feature plots showing the expression levels of selected marker genes used to identify cDC clusters. Black arrows indicate cDC clusters (cluster 6 is cDC2 and cluster 12 is cDC1). (C)

Re-clustering of clusters 6 and 12 corresponding to cDCs. (D) Violin plots referred to clusters in (C) showing expression levels of selected marker genes. (E) Violin plots referred to clusters in (C) showing the number of genes and the number of molecules detected in each cluster. Cluster 8 was identified as doublets and removed. (F) Re-clustering of clusters 0, 1, 2, 3, 4, 5, 6, 7 and 9 from (C). (G) Violin plots referred to clusters in (F) showing expression levels of selected marker genes. Cluster 6, positive for CLEC4C, was identified as contaminant and removed. All other clusters were re-clustered in a final iteration to clearly delineate cDC1, DC2 and DC3 subsets as shown in Figure 2C.

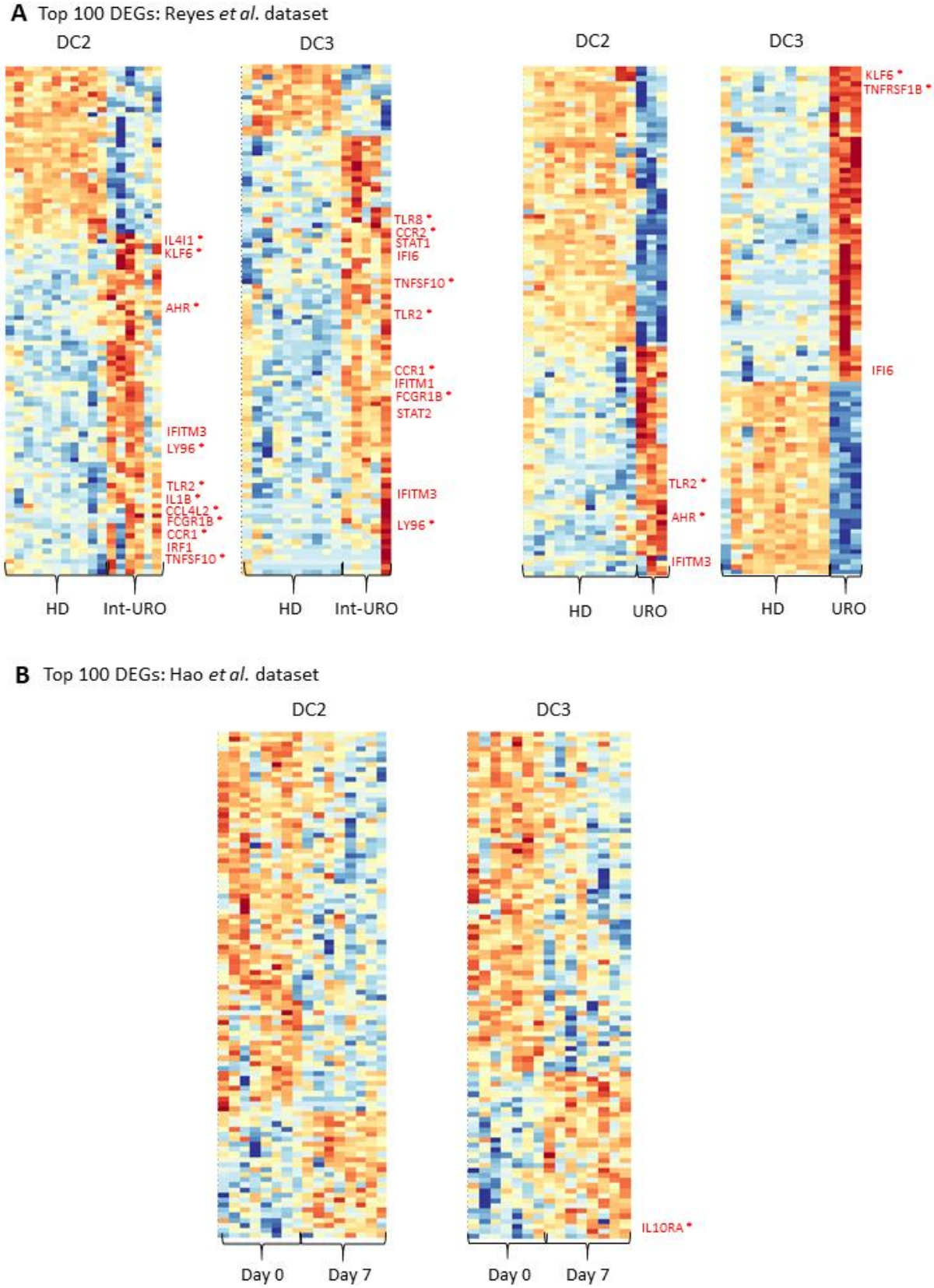

Supplementary Figure 8. Expression heatmaps showing the top 100 DEGs from sepsis and vaccine datasets. Heatmap showing the top 100 DEGs for DC2 and DC3 subsets from (A) Reyes *et al.* and (B) Hao *et al.* datasets. Selected up-regulated genes are marked in red.

Asterisk indicates genes associated with pro-inflammatory functions. Ribosomal protein (RP) genes were removed from the top 100 DEGs. Int-URO, intermediate urosepsis. URO, urosepsis.

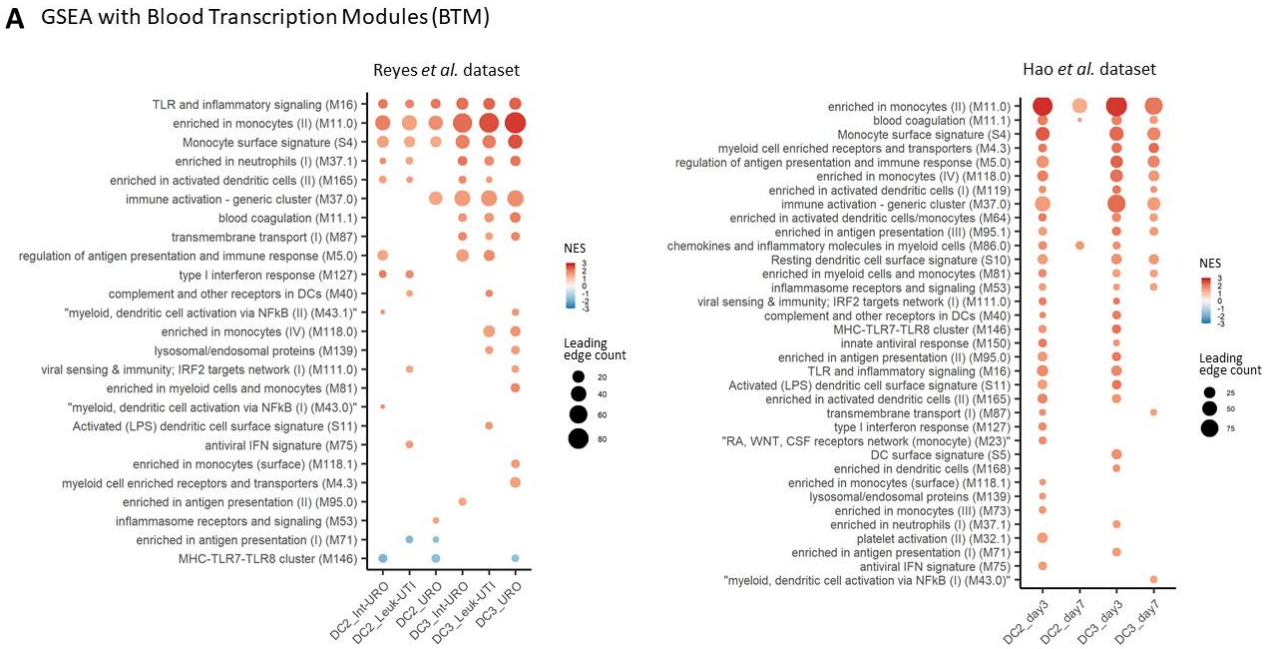

Supplementary Figure 9. GSEA with Blood Transcription Modules (BTM) for Reyes *et al.* and Hao *et al.* datasets. (A) GSEA of DEGs using the BTM collection: Reyes *et al.* dataset (left panel) and Hao *et al.* dataset (right panel). Only pathways with a p-value < 0.05 are shown. Dot size encodes the number of genes in the leading edge. NES, normalized enrichment score. Leuk-UTI, urinary tract infection with leukocytosis. Int-URO, intermediate urosepsis. URO, urosepsis.

Table S1.

sample ID	Disease severity	age	gender	experiment
Covid 1	5, SEVERE	62	female	scRNAseq
Covid 2	4, MILD	66	male	scRNAseq
Covid 3	4 , MILD	68	female	scRNAseq
HD1	N/A	N/A	N/A	scRNAseq
HD2	N/A	N/A	N/A	scRNAseq
Covid 4	5, SEVERE	87	male	DCs frequency analysis
Covid 5	5, SEVERE	68	male	DCs frequency analysis
Covid 6	5, SEVERE	49	male	DCs frequency analysis
Covid 7	4, MILD	79	male	DCs frequency analysis
Covid 8	6, SEVERE	77	male	DCs frequency analysis
Covid 9	4, MILD	60	male	DCs frequency analysis
Covid 10	4, MILD	81	female	DCs frequency analysis
Covid 11	4, MILD	84	male	DCs frequency analysis
Covid 12	4, MILD	67	female	DCs frequency analysis
Covid 13	4, MILD	69	male	DCs frequency analysis
Covid 14	4, MILD	89	female	DCs frequency analysis
Covid 15	6, SEVERE	59	female	DCs frequency analysis
Covid 16	3, MILD	53	male	DCs frequency analysis
Covid 17	3, MILD	89	male	DCs frequency analysis
Covid 18	6, SEVERE	61	male	DCs frequency analysis
Covid 19	4, MILD	80	female	DCs frequency analysis
Covid 20	4, MILD	79	male	DCs frequency analysis
Covid 21	4, MILD	85	female	DCs frequency analysis
Covid 22	4, MILD	59	male	DCs frequency analysis
Covid 23	3, MILD	72	male	DCs frequency analysis
Covid 24	6, SEVERE	62	male	DCs frequency analysis
Covid 25	3, MILD	78	male	DCs frequency analysis
Covid 26	6, SEVERE	68	male	DCs frequency analysis
Covid 27	3, MILD	67	male	DCs frequency analysis
Covid 28	4, MILD	83	female	DCs frequency analysis
Covid 29	6, SEVERE	31	male	DCs frequency analysis
Covid 30	4, MILD	79	male	DCs frequency analysis
Covid 31	4, MILD	80	male	DCs frequency analysis
Covid 32	3, MILD	72	male	DCs frequency analysis
Covid 33	6, SEVERE	65	female	DCs frequency analysis
HD3	N/A	34	female	DCs frequency analysis
HD4	N/A	32	male	DCs frequency analysis
HD5	N/A	27	male	DCs frequency analysis
HD6	N/A	40	female	DCs frequency analysis
HD7	N/A	N/A	N/A	DCs frequency analysis
HD8	N/A	N/A	N/A	DCs frequency analysis
HD9	N/A	N/A	N/A	DCs frequency analysis
HD10	N/A	N/A	N/A	DCs frequency analysis
HD11	N/A	N/A	N/A	DCs frequency analysis
HD12	N/A	N/A	N/A	DCs frequency analysis
HD13	N/A	N/A	N/A	DCs frequency analysis
HD14	N/A	57	female	DCs frequency analysis
HD15	N/A	34	male	DCs frequency analysis
HD16	N/A	41	male	DCs frequency analysis
HD17	N/A	85	male	DCs frequency analysis
HD18	N/A	62	N/A	DCs frequency analysis
HD19	N/A	73	N/A	DCs frequency analysis
HD20	N/A	57	N/A	DCs frequency analysis
HD21	N/A	34	N/A	DCs frequency analysis
HD22	N/A	70	N/A	DCs frequency analysis
HD23	N/A	64	N/A	DCs frequency analysis

Table S1. Characteristics of COVID-19 patients and healthy donors (HD) enrolled in the study.

Table S2. DEGs between COVID-19 patients and healthy donors in each DC subset from datasets 1, 2 and 3.

Table S3. BTM families used for GSEA.

Table S4. DEGs in each DC subset from Reyes *et al.* and Hao *et al.* datasets.

References

1. A. Silvin, N. Chapuis, G. Dunsmore, A. G. Goubet, A. Dubuisson, L. Derosa, C. Almire, C. Hénon, O. Kosmider, N. Droin, P. Rameau, C. Catelain, A. Alfaro, C. Dussiau, C. Friedrich, E. Sourdeau, N. Marin, T. A. Szwebel, D. Cantin, L. Mouthon, D. Borderie, M. Deloger, D. Bredel, S. Mouraud, D. Drubay, M. Andrieu, A. S. Lhonneur, V. Saada, A. Stoclin, C. Willekens, F. Pommeret, F. Griscelli, L. G. Ng, Z. Zhang, P. Bost, I. Amit, F. Barlesi, A. Marabelle, F. Pène, B. Gachot, F. André, L. Zitvogel, F. Ginhoux, M. Fontenay, E. Solary, Elevated Calprotectin and Abnormal Myeloid Cell Subsets Discriminate Severe from Mild COVID-19, *Cell* (2020), doi:10.1016/j.cell.2020.08.002.

2. C. Lucas, P. Wong, J. Klein, T. B. R. Castro, J. Silva, M. Sundaram, M. K. Ellingson, T. Mao, J. E. Oh, B. Israelow, T. Takahashi, M. Tokuyama, P. Lu, A. Venkataraman, A. Park, S. Mohanty, H. Wang, A. L. Wyllie, C. B. F. Vogels, R. Earnest, S. Lapidus, I. M. Ott, A. J. Moore, M. C. Muenker, J. B. Fournier, M. Campbell, C. D. Odio, A. Casanovas-Massana, A. Obaid, A. Lu-Culligan, A. Nelson, A. Brito, A. Nunez, A. Martin, A. Watkins, B. Geng, C. Kalinich, C. Harden, C. Todeasa, C. Jensen, D. Kim, D. McDonald, D. Shepard, E. Courchaine, E. B. White, E. Song, E. Silva, E. Kudo, G. DeIuliis, H. Rahming, H. J. Park, I. Matos, J. Nouws, J. Valdez, J. Fauver, J. Lim, K. A. Rose, K. Anastasio, K. Brower, L. Glick, L. Sharma, L. Sewanan, L. Knaggs, M. Minasyan, M. Batsu, M. Petrone, M. Kuang, M. Nakahata, M. Campbell, M. Linehan, M. H. Askenase, M. Simonov, M. Smolgovsky, N. Sonnert, N. Naushad, P. Vijayakumar, R. Martinello, R. Datta, R. Handoko, S. Bermejo, S. Prophet, S. Bickerton, S. Velazquez, T. Alpert, T. Rice, W. Khoury-Hanold, X. Peng, Y. Yang, Y. Cao, Y. Strong, R. Herbst, A. C. Shaw, R. Medzhitov, W. L. Schulz, N. D. Grubaugh, C. Dela Cruz, S. Farhadian, A. I. Ko, S. B. Omer, A. Iwasaki, Longitudinal analyses reveal immunological misfiring in severe COVID-19, *Nature* (2020), doi:10.1038/s41586-020-2588-y.

3. N. Mangalmurti, C. A. Hunter, Cytokine Storms: Understanding COVID-19*Immunity* (2020), doi:10.1016/j.immuni.2020.06.017.

4. J. T. Merrill, D. Erkan, J. Winakur, J. A. James, Emerging evidence of a COVID-19 thrombotic syndrome has treatment implications*Nature Reviews Rheumatology* (2020), doi:10.1038/s41584-020-0474-5.

5. Z. Wu, J. M. McGoogan, Characteristics of and Important Lessons from the Coronavirus Disease 2019 (COVID-19) Outbreak in China: Summary of a Report of 72314 Cases from the Chinese Center for Disease Control and Prevention*JAMA - Journal of the American Medical Association* (2020), doi:10.1001/jama.2020.2648.

6. A. G. Laing, A. Lorenc, I. del Molino del Barrio, A. Das, M. Fish, L. Monin, M. Muñoz-Ruiz, D. R. McKenzie, T. S. Hayday, I. Francos-Quijorna, S. Kamdar, M. Joseph, D. Davies, R. Davis, A. Jennings, I. Zlatareva, P. Vantourout, Y. Wu, V. Sofra, F. Cano, M. Greco, E. Theodoridis, J. Freedman, S. Gee, J. N. E. Chan, S. Ryan, E. Bugallo-Blanco, P. Peterson, K. Kisand, L. Haljasmägi, L. Chadli, P. Moingeon, L. Martinez, B. Merrick, K. Bisnauthsing, K. Brooks, M. A. A. Ibrahim, J. Mason, F. Lopez Gomez, K. Babalola, S. Abdul-Jawad, J. Cason, C. Mant, J. Seow, C. Graham, K. J. Doores, F. Di Rosa, J. Edgeworth, M. Shankar-Hari, A. C. Hayday, A dynamic COVID-19 immune signature includes associations with poor prognosis, *Nature Medicine* (2020), doi:10.1038/s41591-020-1038-6.

7. M. Cabeza-Cabrerizo, A. Cardoso, C. M. Minutti, M. Pereira da Costa, C. Reis e Sousa, Dendritic Cells Revisited, *Annual Review of Immunology* (2021), doi:10.1146/annurev-immunol-061020-053707.

8. S. C. Eisenbarth, Dendritic cell subsets in T cell programming: location dictates

function*Nature Reviews Immunology* (2019), doi:10.1038/s41577-018-0088-1.

9. P. See, C. A. Dutertre, J. Chen, P. Günther, N. McGovern, S. E. Irac, M. Gunawan, M. Beyer, K. Händler, K. Duan, H. R. Bin Sumatoh, N. Ruffin, M. Jouve, E. Gea-Mallorquí, R. C. M. Hennekam, T. Lim, C. C. Yip, M. Wen, B. Malleret, I. Low, N. B. Shadan, C. F. S. Fen, A. Tay, J. Lum, F. Zolezzi, A. Larbi, M. Poidinger, J. K. Y. Chan, Q. Chen, L. Rénia, M. Haniffa, P. Benaroch, A. Schlitzer, J. L. Schultze, E. W. Newell, F. Ginhoux, Mapping the human DC lineage through the integration of high-dimensional techniques, *Science* (2017), doi:10.1126/science.aag3009.

10. D. A. Anderson, C. A. Dutertre, F. Ginhoux, K. M. Murphy, Genetic models of human and mouse dendritic cell development and function*Nature Reviews Immunology* (2020), doi:10.1038/s41577-020-00413-x.

11. M. Guilliams, C. A. Dutertre, C. L. Scott, N. McGovern, D. Sichien, S. Chakarov, S. Van Gassen, J. Chen, M. Poidinger, S. De Prijck, S. J. Tavernier, I. Low, S. E. Irac, C. N. Mattar, H. R. Sumatoh, G. H. L. Low, T. J. K. Chung, D. K. H. Chan, K. K. Tan, T. L. K. Hon, E. Fossum, B. Bogen, M. Choolani, J. K. Y. Chan, A. Larbi, H. Luche, S. Henri, Y. Saeys, E. W. Newell, B. N. Lambrecht, B. Malissen, F. Ginhoux, Unsupervised High-Dimensional Analysis Aligns Dendritic Cells across Tissues and Species, *Immunity* (2016), doi:10.1016/j.immuni.2016.08.015.

12. J. Canton, H. Blees, C. M. Henry, M. D. Buck, O. Schulz, N. C. Rogers, E. Childs, S. Zelenay, H. Rhys, M. C. Domart, L. Collinson, A. Alloatti, C. J. Ellison, S. Amigorena, V. Papayannopoulos, D. C. Thomas, F. Randow, C. Reis e Sousa, The receptor DNGR-1 signals for phagosomal rupture to promote cross-presentation of dead-cell-associated antigens, *Nature Immunology* (2021), doi:10.1038/s41590-020-00824-x.

13. S. L. Jongbloed, A. J. Kassianos, K. J. McDonald, G. J. Clark, X. Ju, C. E. Angel, C. J. J. Chen, P. R. Dunbar, R. B. Wadley, V. Jeet, A. J. E. Vulink, D. N. J. Hart, K. J. Radford, Human CD141+ (BDCA-3)+ dendritic cells (DCs) represent a unique myeloid DC subset that cross-presents necrotic cell antigens, *Journal of Experimental Medicine* (2010), doi:10.1084/jem.20092140.

14. G. Nizzoli, J. Krietsch, A. Weick, S. Steinfelder, F. Facciotti, P. Gruarin, A. Bianco, B. Steckel, M. Moro, M. Crosti, C. Romagnani, K. Stölzel, S. Torretta, L. Pignataro, C. Scheibenbogen, P. Neddermann, R. De Francesco, S. Abrignani, J. Geginat, Human CD1c+ dendritic cells secrete high levels of IL-12 and potently prime cytotoxic T-cell responses, *Blood* (2013), doi:10.1182/blood-2013-04-495424.

15. C. Ad. Utertre, E. Becht, S. E. Irac, A. Khalilnezhad, V. Narang, S. Khalilnezhad, P. Y. Ng, L. L. van den Hoogen, J. Y. Leong, B. Lee, M. Chevrier, X. M. Zhang, P. J. A. Yong, G. Koh, J. Lum, S. W. Howland, E. Mok, J. Chen, A. Larbi, H. K. K. Tan, T. K. H. Lim, P. Karagianni, A. G. Tzioufas, B. Malleret, J. Brody, S. Albani, J. van Roon, T. Radstake, E. W. Newell, F. Ginhoux, Single-Cell Analysis of Human Mononuclear Phagocytes Reveals Subset-Defining Markers and Identifies Circulating Inflammatory Dendritic Cells, *Immunity* (2019), doi:10.1016/j.immuni.2019.08.008.

16. A. C. Villani, R. Satija, G. Reynolds, S. Sarkizova, K. Shekhar, J. Fletcher, M. Griesbeck, A. Butler, S. Zheng, S. Lazo, L. Jardine, D. Dixon, E. Stephenson, E. Nilsson, I. Grundberg, D. McDonald, A. Filby, W. Li, P. L. De Jager, O. Rozenblatt-Rosen, A. A. Lane, M. Haniffa, A. Regev, N. Hacohen, Single-cell RNA-seq reveals new types of human blood dendritic cells, monocytes, and progenitors, *Science* (2017), doi:10.1126/science.aah4573.

17. U. Cytlak, A. Resteu, S. Pagan, K. Green, P. Milne, S. Maisuria, D. McDonald, G.

Hulme, A. Filby, B. Carpenter, R. Queen, S. Hambleton, R. Hague, H. Lango Allen, J. E. D. Thaventhiran, G. Doody, M. Collin, V. Bigley, Differential IRF8 Transcription Factor Requirement Defines Two Pathways of Dendritic Cell Development in Humans, *Immunity* (2020), doi:10.1016/j.immuni.2020.07.003.

18. I. Sánchez-Cerrillo, P. Landete, B. Aldave, S. Sánchez-Alonso, A. Sánchez-Azofra, A. Marcos-Jiménez, E. Ávalos, A. Alcaraz-Serna, I. de los Santos, T. Mateu-Albero, L. Esparcia, C. López-Sanz, P. Martínez-Fleta, L. Gabrie, L. del Campo Guerola, H. de la Fuente, M. J. Calzada, I. González-Álvaro, A. Alfranca, F. Sánchez-Madrid, C. Muñoz-Calleja, J. B. Soriano, J. Ancochea, E. Martín-Gayo, COVID-19 severity associates with pulmonary redistribution of CD1c+ DCs and inflammatory transitional and nonclassical monocytes, *Journal of Clinical Investigation* (2020), doi:10.1172/JCI140335.

19. E. Kvedaraite, L. Hertwig, I. Sinha, A. Ponzetta, I. Hed Myrberg, M. Lourda, M. Dzidic, M. Akber, J. Klingström, E. Folkesson, J. R. Muvva, P. Chen, S. Gredmark-Russ, S. Brighenti, A. Norrby-Teglund, L. I. Eriksson, O. Rooyackers, S. Aleman, K. Strålin, H.-G. Ljunggren, F. Ginhoux, N. K. Björkström, J.-I. Henter, M. Svensson, Major alterations in the mononuclear phagocyte landscape associated with COVID-19 severity, *Proceedings of the National Academy of Sciences* (2021), doi:10.1073/pnas.2018587118.

20. R. Zhou, K. K. W. To, Y. C. Wong, L. Liu, B. Zhou, X. Li, H. Huang, Y. Mo, T. Y. Luk, T. T. K. Lau, P. Yeung, W. M. Chan, A. K. L. Wu, K. C. Lung, O. T. Y. Tsang, W. S. Leung, I. F. N. Hung, K. Y. Yuen, Z. Chen, Acute SARS-CoV-2 Infection Impairs Dendritic Cell and T Cell Responses, *Immunity* (2020), doi:10.1016/j.immuni.2020.07.026.

21. A. Sette, S. Crotty, Adaptive immunity to SARS-CoV-2 and COVID-19*Cell* (2021), doi:10.1016/j.cell.2021.01.007.

22. P. S. Arunachalam, F. Wimmers, C. K. P. Mok, R. A. P. M. Perera, M. Scott, T. Hagan, N. Sigal, Y. Feng, L. Bristow, O. T. Y. Tsang, D. Wagh, J. Coller, K. L. Pellegrini, D. Kazmin, G. Alaaeddine, W. S. Leung, J. M. C. Chan, T. S. H. Chik, C. Y. C. Choi, H. CHuerta, M. P. McCullough, H. Lv, E. Anderson, S. Edupuganti, A. A. Upadhyay, S. E. Bosinger, H. Terry, P. Khatri, N. Rouphael, M. Peiris, B. Pulendran, Systems biological assessment of immunity to mild versus severe COVID-19 infection in humans, *Science* (2020), doi:10.1126/SCIENCE.ABC6261.

23. J. Schulte-Schrepping, N. Reusch, D. Paclik, K. Baßler, S. Schlickeiser, B. Zhang, B. Krämer, T. Krammer, S. Brumhard, L. Bonaguro, E. De Domenico, D. Wendisch, M. Grasshoff, T. S. Kapellos, M. Beckstette, T. Pecht, A. Saglam, O. Dietrich, H. E. Mei, A. R. Schulz, C. Conrad, D. Kunkel, E. Vafadarnejad, C. J. Xu, A. Horne, M. Herbert, A. Drews, C. Thibeault, M. Pfeiffer, S. Hippenstiel, A. Hocke, H. Müller-Redetzky, K. M. Heim, F. Machleidt, A. Uhrig, L. Bosquillon de Jarcy, L. Jürgens, M. Stegemann, C. R. Glösenkamp, H. D. Volk, C. Goffinet, M. Landthaler, E. Wyler, P. Georg, M. Schneider, C. Dang-Heine, N. Neuwinger, K. Kappert, R. Tauber, V. Corman, J. Raabe, K. M. Kaiser, M. T. Vinh, G. Rieke, C. Meisel, T. Ulas, M. Becker, R. Geffers, M. Witzenrath, C. Drosten, N. Suttorp, C. von Kalle, F. Kurth, K. Händler, J. L. Schultze, A. C. Aschenbrenner, Y. Li, J. Nattermann, B. Sawitzki, A. E. Saliba, L. E. Sander, A. Angelov, R. Bals, A. Bartholomäus, A. Becker, D. Bezdan, E. Bonifacio, P. Bork, T. Clavel, M. Colome-Tatche, A. Diefenbach, A. Dilthey, N. Fischer, K. Förstner, J. S. Frick, J. Gagneur, A. Goesmann, T. Hain, M. Hummel, S. Janssen, J. Kalinowski, R. Kallies, B. Kehr, A. Keller, S. Kim-Hellmuth, C. Klein, O. Kohlbacher, J. O. Korbel, I. Kurth, K. Ludwig, O. Makarewicz, M. Marz, A. McHardy, C. Mertes, M. Nöthen, P. Nürnberg, U. Ohler, S. Ossowski, J. Overmann, S. Peter, K. Pfeffer, A. R. Poetsch, A. Pühler, N. Rajewsky, M. Ralser, O. Rieß, S. Ripke, U. Nunes da Rocha, P.

Rosenstiel, P. Schiffer, E. C. Schulte, A. Sczyrba, O. Stegle, J. Stoye, F. Theis, J. Vehreschild, J. Vogel, M. von Kleist, A. Walker, J. Walter, D. Wieczorek, J. Ziebuhr, Severe COVID-19 Is Marked by a Dysregulated Myeloid Cell Compartment, *Cell* (2020), doi:10.1016/j.cell.2020.08.001.

24. S. Li, N. Rouphael, S. Duraisingham, S. Romero-Steiner, S. Presnell, C. Davis, D. S. Schmidt, S. E. Johnson, A. Milton, G. Rajam, S. Kasturi, G. M. Carlone, C. Quinn, D. Chaussabel, A. K. Palucka, M. J. Mulligan, R. Ahmed, D. S. Stephens, H. I. Nakaya, B. Pulendran, Molecular signatures of antibody responses derived from a systems biology study of five human vaccines, *Nature Immunology* (2014), doi:10.1038/ni.2789.

25. M. Reyes, M. R. Filbin, R. P. Bhattacharyya, K. Billman, T. Eisenhaure, D. T. Hung, B. D. Levy, R. M. Baron, P. C. Blainey, M. B. Goldberg, N. Hacohen, An immune-cell signature of bacterial sepsis*Nature Medicine* (2020), doi:10.1038/s41591-020-0752-4.

26. Y. Hao, S. Hao, E. Andersen-Nissen, W. M. Mauck, S. Zheng, A. Butler, M. J. Lee, A. J. Wilk, C. Darby, M. Zagar, P. Hoffman, M. Stoeckius, E. Papalexi, E. P. Mimitou, J. Jain, A. Srivastava, T. Stuart, L. B. Fleming, B. Yeung, A. J. Rogers, J. M. McElrath, C. A. Blish, R. Gottardo, P. Smibert, R. Satija, Integrated analysis of multimodal single-cell data*bioRxiv* (2020), doi:10.1101/2020.10.12.335331.

27. S. S. Pullamsetti, W. Seeger, R. Savai, Classical IL-6 signaling: A promising therapeutic target for pulmonary arterial hypertension*Journal of Clinical Investigation* (2018), doi:10.1172/JCI120415.

28. J. Zheng, Y. Wang, K. Li, D. K. Meyerholz, C. Allamargot, S. Perlman, Severe Acute Respiratory Syndrome Coronavirus 2–Induced Immune Activation and Death of Monocyte-Derived Human Macrophages and Dendritic Cells, *The Journal of Infectious Diseases* (2020), doi:10.1093/infdis/jiaa753.

29. P. Bourdely, G. Anselmi, K. Vaivode, R. N. Ramos, Y. Missolo-Koussou, S. Hidalgo, J. Tosselo, N. Nuñez, W. Richer, A. Vincent-Salomon, A. Saxena, K. Wood, A. Lladser, E. Piaggio, J. Helft, P. Guermonprez, Transcriptional and Functional Analysis of CD1c+ Human Dendritic Cells Identifies a CD163+ Subset Priming CD8+CD103+ T Cells, *Immunity* (2020), doi:10.1016/j.immuni.2020.06.002.

30. T. Vogl, A. Stratis, V. Wixler, T. Völler, S. Thurainayagam, S. K. Jorch, S. Zenker, A. Dreiling, D. Chakraborty, M. Fröhling, P. Paruzel, C. Wehmeyer, S. Hermann, O. Papantonopoulou, C. Geyer, K. Loser, M. Schäfers, S. Ludwig, M. Stoll, T. Leanderson, J. L. Schultze, S. König, T. Pap, J. Roth, Autoinhibitory regulation of S100A8/S100A9 alarmin activity locally restricts sterile inflammation, *Journal of Clinical Investigation* (2018), doi:10.1172/JCI89867.

31. G. Bakdash, S. I. Buschow, M. A. J. Gorris, A. Halilovic, S. V. Hato, A. E. Sköld, G. Schreibelt, S. P. Sittig, R. Torensma, T. Duiveman-De Boer, C. Schröder, E. L. Smits, C. G. Figdor, I. J. M. De Vries, Expansion of a BDCA1+ CD14+ myeloid cell population in melanoma patients may attenuate the efficacy of dendritic cell vaccines, *Cancer Research* (2016), doi:10.1158/0008-5472.CAN-15-1695.

32. A. T. Tan, M. Linster, C. W. Tan, N. Le Bert, W. N. Chia, K. Kunasegaran, Y. Zhuang, C. Y. L. Tham, A. Chia, G. J. D. Smith, B. Young, S. Kalimuddin, J. G. H. Low, D. Lye, L. F. Wang, A. Bertoletti, Early induction of functional SARS-CoV-2-specific T cells associates with rapid viral clearance and mild disease in COVID-19 patients, *Cell Reports* (2021), doi:10.1016/j.celrep.2021.108728.

33. C. Hafemeister, R. Satija, Normalization and variance stabilization of single-cell RNA-seq data using regularized negative binomial regression, *Genome Biol.* (2019), doi:10.1186/s13059-019-1874-1.

34. I. Korsunsky, N. Millard, J. Fan, K. Slowikowski, F. Zhang, K. Wei, Y. Baglaenko, M. Brenner, P. ru Loh, S. Raychaudhuri, Fast, sensitive and accurate integration of single-cell data with Harmony, *Nat. Methods* (2019), doi:10.1038/s41592-019-0619-0.

35. M. D. Robinson, D. J. McCarthy, G. K. Smyth, edgeR: A Bioconductor package for differential expression analysis of digital gene expression data, *Bioinformatics* (2009), doi:10.1093/bioinformatics/btp616.

36. A. Subramanian, P. Tamayo, V. K. Mootha, S. Mukherjee, B. L. Ebert, M. A. Gillette, A. Paulovich, S. L. Pomeroy, T. R. Golub, E. S. Lander, J. P. Mesirov, Gene set enrichment analysis: A knowledge-based approach for interpreting genome-wide expression profiles, *Proc. Natl. Acad. Sci. U. S. A.* (2005), doi:10.1073/pnas.0506580102.

37. A. A. Sergushichev, An algorithm for fast preranked gene set enrichment analysis using cumulative statistic calculation, *bioRxiv* (2016).

38. A. Liberzon, C. Birger, H. Thorvaldsdóttir, M. Ghandi, J. P. Mesirov, P. Tamayo, The Molecular Signatures Database Hallmark Gene Set Collection, *Cell Syst.* (2015), doi:10.1016/j.cels.2015.12.004.